GUIDED ELECTROMAGNETIC WAVES IN ANISOTROPIC MEDIA

PROEFSCHRIFT

TER VERKRIJGING VAN DE GRAAD VAN DOCTOR IN DE TECHNISCHE WETENSCHAP AAN DE TECHNISCHE HOGESCHOOL TE DELFT, OP GEZAG VAN DE RECTOR MAGNIFICUS DR O. BOTTEMA, HOOGLERAAR IN DE AFDELING DER ALGEMENE WETENSCHAPPEN, VOOR EEN COMMISSIE UIT DE SENAAT TE VERDEDIGEN OP WOENSDAG 16 DECEMBER 1953 DES NAMIDDAGS TE 4 UUR

DOOR

ANTONIUS ARNOLDUS THEODORUS MARIA VAN TRIER

ELECTROTECHNISCH INGENIEUR, GEBOREN TE OSS

'S-GRAVENHAGE
MARTINUS NIJHOFF
1953

Dit proefschrift is goedgekeurd door de promotor

PROF. DR R. KRONIG

AAN MIJN OUDERS

Het onderzoek, dat in dit proefschrift beschreven wordt, is uitgevoerd in het Physisch Laboratorium van de Rijksverdedigingsorganisatie T.N.O. Aan het bestuur van de Rijksverdedigingsorganisatie, dat mij toestemming heeft willen verlenen tot het publiceren van de resultaten van dit onderzoek, betuig ik mijn hartelijke dank.

SAMENVATTING

Dit proefschrift heeft tot onderwerp de voortplanting van geleide electromagnetische golven in anisotrope media. Dit probleem is in twee tamelijk uiteenlopende gebieden van onderzoek naar voren gekomen, nl. bij ferromagnetische resonantie-experimenten en bij het onderzoek van de magnetische Faradayrotatie van geleide golven in ferromagnetische ferrieten. In beide gevallen moet een oplossing gevonden worden van de vergelijkingen van Maxwell in een ruimte, die begrensd is door oneindig goed geleidende wanden en die geheel of gedeeltelijk gevuld is met een medium, waarvan de magnetische permeabiliteit door een tensor beschreven wordt.

Hoofdstuk I is een algemene inleiding. Na een korte samenvatting van enkele belangrijke resultaten uit de theorie van geleide golven in isotrope media worden, uitgaande van de algemene beschouwingen van Tellegen betreffende anisotrope media, gyromagnetische en gyroëlectrische media gedefinieerd. Ook wordt een kort historisch overzicht gegeven van het theoretische en experimentele werk, dat op dit gebied is verricht. Voor de theoretische beschouwingen, die Hoofdstuk II vormen, wordt als uitgangspunt een golfgeleider van willekeurige doorsnede genomen, die het algemene anisotrope medium van Tellegen bevat. Veel aandacht wordt besteed aan het speciale geval, dat dit medium gyromagnetisch en gyroëlectrisch is. Als toepassingen worden golfgeleiders behandeld, die bestaan uit twee evenwijdige vlakke platen, en golfgeleiders van ronde doorsnede. De laatste configuratie is van belang met het oog op metingen van magnetische Faradayrotatie. In Hoofdstuk III wordt een methode beschreven om Faradayrotaties van geleide golven te meten in een trilholte. Tevens wordt aangegeven hoe de Q-factor van een trilholte bepaald kan worden uit reflectiemetingen, waarbij in het bijzonder het koppelingsprobleem belicht wordt. Hoofdstuk IV bevat de resultaten van de metingen, die verricht zijn aan de Ferroxcuben IV bij een frequentie van 24000 MHz. In Hoofdstuk V wordt de theorie van de permeabiliteitstensor enigszins uitgebreid. Tenslotte worden de experimentele resultaten vergeleken met de theoretische, waarbij blijkt, dat de overeenstemming goed is.

CONTENTS

GUIDED ELECTROMAGNETIC WAVES IN ANISOTROPIC MEDIA

Summary

The propagation of guided waves in anisotropic media has recently become of interest in two fields, viz. in the interpretation of ferromagnetic resonance experiments and in the construction of microwave fourpoles which violate the reciprocity relation. In both cases we are faced with the solution of Maxwell's equations in a volume which is enclosed by perfectly conducting walls and which is completely or partially filled with a medium whose magnetic permeability is described by a second order tensor. An account is given here of some work, both theoretical and experimental, on this subject. Chapter I is an introduction, containing a short survey of the theory of guided waves in isotropic media and of the problems arising in anisotropic media, together with a historical synopsis. Chapter II gives a general formulation of the theory of guided waves in anisotropic media, comprising the existing theories, and also deals with some new applications. In Chapter III a cavity technique for measuring Faraday rotations is described which has several advantages over older techniques. In Chapter IV experimental results obtained for the series of Ferroxcubes IVA, B, C, D, E are collected. Chapter V finally deals with the physical interpretation of these results. In particular the experimental data are compared with Rado's theory of the permeability tensor in non-saturated ferromagnetics.

CHAPTER I. INTRODUCTION

§ 1. *General remarks.* Before we deal with our subject proper, propagation of guided waves in anisotropic media, it seems appropriate to summarize the main results of the theory of guided waves in isotropic media, as it may be expected that many characteristics will be the same for both cases. Let us first of all indicate some conventions and restrictions which will be adhered to throughout the following pages:

a) The wave guides are supposed to consist of cylinders with cross-sections of arbitrary form, the walls being perfect conductors.

b) Unless stated otherwise all media inside the wave guides are assumed to be homogeneous, linear and without dissipation.

c) Generalized orthogonal cylindrical coordinates v_1, v_2, z are used to describe the fields within the wave guides: v_1 and v_2 determine the position of a point in the cross-section, the z-axis is taken parallel to the axis of the wave guide. The unit vectors in the v_1, v_2 and z-directions are $\mathbf{i}_1$, $\mathbf{i}_2$ and $\mathbf{k}$, the line elements in these directions $h_1\,dv_1$, $h_2\,dv_2$ and dz, where h_1 and h_2 are functions of v_1 and v_2. In summations the indices v_1, v_2, z will occasionally be replaced by the numbers 1, 2, 3.

d) The field components vary harmonically with time; this may be represented by time factors $\exp j\omega t$ which usually will be omitted.

e) Rationalized MKS units will be used.

On account of *b*) and *d*) Maxwell's equations may be written in the form

$$\nabla \times \mathbf{E} = -j\omega\mathbf{B}, \quad \nabla \times \mathbf{H} = j\omega\mathbf{D}. \tag{1.1}$$

From these equations we find at once

$$\nabla \cdot \mathbf{D} = 0, \ \nabla \cdot \mathbf{B} = 0. \tag{1.2}$$

In isotropic media we have the additional relations

$$\mathbf{D} = \varepsilon\mathbf{E}, \ \mathbf{B} = \mu\mathbf{H}. \tag{1.3}$$

In accordance with *b*) ε and μ are assumed to be real. Wave equations for $\mathbf{E}$ and $\mathbf{H}$ can be derived at once from (1), (2) and (3):

$$\nabla^2\mathbf{E} + \omega^2\varepsilon\mu\mathbf{E} = 0, \ \nabla^2\mathbf{H} + \omega^2\varepsilon\mu\mathbf{H} = 0. \tag{1.4}$$

When the medium is of infinite extent, plane waves may be propagated freely in all directions. For waves, propagated in the direction of a unit vector $\mathbf{n}$, the field components contain the factor exp $(-\gamma_f\mathbf{n}\cdot\mathbf{r})$, where γ_f is given by

$$\gamma_f = j\omega\sqrt{\varepsilon\mu} = j2\pi/\lambda_f. \tag{1.5}$$

The ratio of the amplitudes of the electric and magnetic fields is a constant Z_f, called the wave impedance of the medium

$$Z_f = \sqrt{\mu/\varepsilon}. \tag{1.6}$$

In the case of guided waves, however, the situation is quite different. Now the solutions are of the form

$$\mathbf{E} = \mathbf{E}(v_1, v_2) \exp(-\gamma z), \ \mathbf{H} = \mathbf{H}(v_1, v_2) \exp(-\gamma z), \tag{1.7}$$

where $\mathbf{E}(v_1, v_2)$ is a solution of the equation

$$\nabla_t^2\mathbf{E} + (\gamma^2 - \gamma_f^2)\,\mathbf{E} = 0 \tag{1.8}$$

and similarly for $\mathbf{H}(v_1, v_2)$; by ∇_t^2 we mean the transverse part of the

Laplacean operator, i.e. $\nabla_t^2 \equiv \nabla^2 - \partial^2/\partial z^2$. Moreover **E** and **H** must satisfy certain boundary conditions on the wave guide wall (the tangential component of **E** and the normal component of **H** must disappear), and as a consequence of this (8) has acceptable solutions only for certain discrete values of

$$\gamma^2 - \gamma_f^2 = -\gamma_c^2 = \beta_c^2. \tag{1.9}$$

As a matter of fact there are two infinite series of solutions, called transverse magnetic (TM) modes, and transverse electric (TE) modes, characterized by $H_z = 0$, c.q. $E_z = 0$. The quantities $\gamma_c = j2\pi/\lambda_c$ are called cutoff propagation constants, as they determine the longest wavelength λ_c which can be propagated along the wave guide without attenuation. This is an immediate consequence of (9) which may be written as

$$\gamma^2 = (2\pi/\lambda_c)^2 - (2\pi/\lambda_f)^2. \tag{1.9a}$$

Now it is clear that

$$\gamma^2 < 0, \text{ if } \lambda_f < \lambda_c\text{: wave propagation,}$$
$$\gamma^2 = 0, \text{ if } \lambda_f = \lambda_c\text{: cutoff,}$$
$$\gamma^2 > 0, \text{ if } \lambda_f > \lambda_c\text{: exponential attenuation.}$$

In general the β_c's are arranged in order of increasing magnitude: being distinguished as β'_{cn} and β''_{cn} in the case of TM- and TE-modes respectively, with $n = 1, 2, 3, \ldots$. The two series are different in general; only in the special cases of guided waves between two parallel planes of infinite extent and in wave guides of rectangular cross-section they are identical.

It can be proved easily that the TM- and TE-modes have certain orthogonality properties, and it is usually assumed without proof that they form a complete set of solutions. Then the general solution of Maxwell's equations in our configuration consists of a linear superposition of TM- and TE-modes with arbitrary amplitudes. We finally give some expressions for the fields in the various modes; resolving the field vectors into transverse and longitudinal components the following relations hold:

a) TM-m o d e s

$$\left.\begin{aligned} &E_{zn} \neq 0,\ H_{zn} = 0,\\ &\mathbf{E}_{tn} = -(\gamma'_n/\beta'^2_{cn})\,\nabla_t E_{zn}, \qquad Z'_n\,\mathbf{H}_{tn} = \mathbf{k} \times \mathbf{E}_{tn},\\ &Z'_n = \gamma'_n/j\omega\varepsilon. \end{aligned}\right\} \tag{1.10}$$

Here E_{zn} is a solution of $\nabla_t^2 E_z + \beta'^2_{cn} E_z = 0$; the constants β'_{cn} are determined by the boundary condition that $E_z = 0$ on the wall.

Clearly $\nabla_t E_{zn}$ is normal to the wall, and on account of (10) then also $\mathbf{E}_{tn}$ is normal to the wall, as it should be.

b) TE-modes.

Zie college dictaat Kronig I.

$$\left.\begin{aligned} &E_{zn} = 0;\ H_{zn} \neq 0, \\ &\mathbf{E}_{tn} = (j\omega\mu/\beta''^2_{cn})\ \mathbf{k} \times \nabla_t H_{zn},\ Z''_n \mathbf{H}_{tn} = \mathbf{k} \times \mathbf{E}_{tn}, \\ &Z''_n \ = j\omega\mu/\gamma''_n. \end{aligned}\right\} \tag{1.11}$$

Now H_{zn} is a solution of $\nabla_t^2 H_z + \beta''^2_{cn} H_z = 0$, and the constants β''_{cn} are determined by the boundary condition that $\partial H_z/\partial \nu = 0$ at the wall ($\boldsymbol{\nu}$ is the unit vector normal to the wall). In the same way as under *a*) it can be shown that if $\partial H_z/\partial \nu = 0$ at the wall, the tangential component of $\mathbf{E}_t$ disappears simultaneously.

§ 2. *Anisotropic media.* We call a medium anisotropic when either its electric or its magnetic polarizability, or both, are not the same in all directions. The differences may be inherent in non-regular crystal structure, as is the case in crystal optics, or they may be due to constant electric or magnetic fields acting on the medium, as is the case in such optical effects as the Faraday rotation, the Cotton-Mouton effect and the Kerr effect, cf. Voigt[34]). In optics, however, always plane wave propagation is considered. We now ask, from a purely phenomenological point of view, what are the most general relations between the electric and magnetic inductions $\mathbf{D}$ and $\mathbf{B}$ on the one hand, and the electric and magnetic field strengths $\mathbf{E}$ and $\mathbf{H}$ on the other. This question has been investigated by Tellegen[30]). In order to be quite general we must assume that electric polarization can be caused not only by an electric field, but also by a magnetic field, and similarly that an electric field can also contribute to magnetic polarization. We are thus led to the following relations which describe the dielectric and magnetic properties of the most general linear medium, which we henceforth shall call ,,Tellegen's medium'':

$$D_k = \sum_{l=1}^{3} (\varepsilon_{kl} E_l + \xi_{kl} H_l),\quad B_k = \sum_{l=1}^{3} (\zeta_{kl} E_l + \mu_{kl} H_l),\ k = 1, 2, 3. \tag{1.12}$$

Tellegen also investigated what are the conditions for this medium to be without dissipation. He found that the following relations have to be fulfilled:

$$\varepsilon_{kk}, \mu_{kk} \text{ real},\ \varepsilon_{kl} = \varepsilon^*_{lk};\ \mu_{kl} = \mu^*_{lk},\ \xi_{kl} = \zeta^*_{lk}. \tag{1.13}$$

(Here ε^*_{kl} is the complex conjugate of ε_{kl}, etc.).

It is to be noted that in most cases of anisotropy the coefficients ε_{kl} etc. are independent of the coordinates only in rectangular coordinates. In special cases, however, f.i. when the anisotropy is due to external fields, this independence may also hold in other orthogonal coordinate systems.

G y r o m a g n e t i c a n d g y r o e l e c t r i c m e d i a. In Chapter II we shall study rather carefully propagation through a medium for which all ξ_{kl} and ζ_{kl} vanish, and for which the dielectric and magnetic tensors have the form

$$||\varepsilon|| = \begin{Vmatrix} \varepsilon_1 & -j\varepsilon_2 & 0 \\ j\varepsilon_2 & \varepsilon_1 & 0 \\ 0 & 0 & \varepsilon_3 \end{Vmatrix}, \quad ||\mu|| = \begin{Vmatrix} \mu_1 & -j\mu_2 & 0 \\ j\mu_2 & \mu_1 & 0 \\ 0 & 0 & \mu_3 \end{Vmatrix}, \tag{1.14}$$

where ε_i, μ_i, $i = 1, 2, 3$, are real and independent of the coordinates. Such media can be obtained by applying a constant magnetic field in the z-direction to certain isotropic materials. For reasons to be given later a medium whose magnetic properties are described by the μ-tensor (14) is called gyromagnetic, and the direction of the constant magnetic field is denoted as the gyro-axis. Similarly we might call a medium with the ε-tensor of (14) gyroelectric. In view of the relations (13) it is clear that the medium (14) has no dissipation.

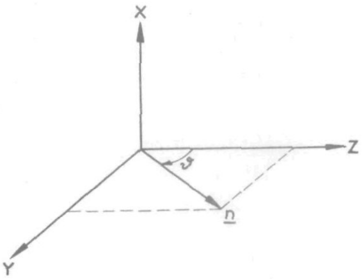

Fig. 1. Coordinate system and direction of propagation.

In Chapter V we shall go into the physical interpretation of the μ-tensor, which is mainly due to P o l d e r [17]. For the moment we shall confine ourselves to indicating which plane waves can be propagated in the medium (14). Let us consider a wave which is propagated in the direction of a unit vector $\mathbf{n}$ making an angle ϑ with the gyro-axis. Then all field components contain the factor exp $(-\gamma \mathbf{n}\cdot\mathbf{r})$, where γ is the propagation constant of the wave. Using rectangular coordinates we may assume without loss of generality that $\mathbf{n}$ lies in the yz-plane. Then $\mathbf{n} = \mathbf{j} \sin \vartheta + \mathbf{k} \cos \vartheta$ (fig. 1). From Maxwell's equations we may derive that γ must satisfy the biquadratic equation

$$\gamma^4 \left(\sin^2 \vartheta + \frac{\mu_3}{\mu_1} \cos^2 \vartheta\right)\left(\sin^2 \vartheta + \frac{\varepsilon_3}{\varepsilon_1} \cos^2 \vartheta\right) + \\ + \gamma^2 \left[\left(\sin^2 \vartheta + \frac{\mu_3}{\mu_1} \cos^2 \vartheta\right) \omega^2 \varepsilon_3 \frac{\mu_1^2 - \mu_2^2}{\mu_1} + \right. \\ \left. + \left(\sin^2 \vartheta + \frac{\varepsilon_3}{\varepsilon_1} \cos^2 \vartheta\right) \omega^2 \frac{\varepsilon_1^2 - \varepsilon_2^2}{\varepsilon_1} \mu_3 + \omega^2 \varepsilon_3 \mu_3 \left(\frac{\varepsilon_2}{\varepsilon_1} + \frac{\mu_2}{\mu_1}\right)^2 \cos^2 \vartheta\right] \\ + \omega^4 \varepsilon_3 \mu_3 \frac{\varepsilon_1^2 - \varepsilon_2^2}{\varepsilon_1} \frac{\mu_1^2 - \mu_2^2}{\mu_1} = 0. \tag{1.15}$$

For each direction $\mathbf{n}$ we find two values of γ^2, and these propagation constants correspond to elliptically polarized waves. It is interesting to consider the special cases $\vartheta = 0$ and $\vartheta = \pi/2$.

a) $\vartheta = 0$. In this case (15) reduces to

$$\gamma^4 + 2\gamma^2 \omega^2 (\varepsilon_1 \mu_1 + \varepsilon_2 \mu_2) + \omega^4 (\varepsilon_1^2 - \varepsilon_2^2)(\mu_1^2 - \mu_2^2) = 0 \tag{1.16}$$

with solutions

$$\gamma_+^2 = - \omega^2 (\varepsilon_1 + \varepsilon_2)(\mu_1 + \mu_2), \quad \gamma_-^2 = - \omega^2 (\varepsilon_1 - \varepsilon_2)(\mu_1 - \mu_2). \tag{1.17}$$

The waves corresponding to $\gamma_{+,-}$ can be shown to be transverse electromagnetic (TEM) and right, c.q. left circularly polarized. Superposition of a right and a left circularly polarized wave of equal amplitudes results in a linearly polarized wave whose direction of polarization rotates about the direction of propagation. This effect is nothing but Faraday rotation, and the Faraday rotation per unit length Θ is found to be

$$\Theta = \tfrac{1}{2}(\beta_+ - \beta_-), \tag{1.18}$$

where $\gamma_+ = j\beta_+$ and $\gamma_- = j\beta_-$. It is well to mention here that the optical Faraday rotation ($\varepsilon_2 \neq 0$, $\mu_2 = 0$) is very small as $\varepsilon_2 \ll \varepsilon_1$, whereas magnetic Faraday rotation in the microwave region ($\varepsilon_2 = 0$, $\mu_2 \neq 0$) can have considerable values as μ_2 may become of the same order of magnitude as μ_1.

b) $\vartheta = \pi/2$. Now (15) reduces to

$$\gamma^4 + \gamma^2 \omega^2 \left(\varepsilon_3 \frac{\mu_1^2 - \mu_2^2}{\mu_1} + \frac{\varepsilon_1^2 - \varepsilon_2^2}{\varepsilon_1} \mu_3\right) + \omega^4 \varepsilon_3 \mu_3 \frac{\varepsilon_1^2 - \varepsilon_2^2}{\varepsilon_1} \frac{\mu_1^2 - \mu_2^2}{\mu_1} = 0 \tag{1.19}$$

free space

with solutions

$-\omega^2\left(\varepsilon_1 - \frac{\varepsilon_2^2}{\varepsilon_1}\right)$

$$\gamma_1^2 = -\,\omega^2 \frac{\varepsilon_1^2 - \varepsilon_2^2}{\varepsilon_1}\mu_3, \qquad \gamma_2^2 = -\,\omega^2\, \varepsilon_3 \frac{\mu_1^2 - \mu_2^2}{\mu_1}. \tag{1.20}$$

It can be verified that γ_1 corresponds to a TM-wave with components E_x, E_y and H_z, and γ_2 to a TE-wave with components H_x, H_y and E_z. These waves can be said to show the electric, c.q. magnetic Cotton-Mouton effect.

§ 3. *Historical survey.* In this section we shall try to give a short account of the work which has been done in the field of guided waves in anisotropic media, both theoretically and experimentally.

Theoretical work. Some researches have been carried out in connection with the Faraday rotation of guided waves in a gyromagnetic medium in wave guides of circular cross-section (the gyro-axis is understood to coincide with the axis of the wave guide). Suhl and Walker [29]) showed that in this case only circularly polarized modes exist, in which both $E_z \neq 0$ and $H_z \neq 0$; i.e. TM- and TE-modes do no longer occur. The same conclusions were reached independently by Gamo [7]), who gave a somewhat more detailed analysis of this configuration. Kales [13]) considered the same problem more generally and derived some results concerning propagation in wave guides of arbitrary cross-section containing gyromagnetic media. The case of a rectangular wave guide, together with a particular boundary value problem arising from it, was studied by van Trier [31]); here the gyro-axis was taken parallel to the narrow side and perpendicular to the longitudinal axis of the wave guide. An investigation of input impedances of cavities containing generalized media is being undertaken by Berk and Lax [3])[4]), but only a few results of their work are available as yet. They give an extension of Slater's theory of impedances of cavities containing isotropic media [26]). An interesting contribution is due to Hafner [10]), who made some computations on cavities filled with anisotropic dielectrics. He considered the possibility of measuring the main dielectric constants of crystals. By far the most general approach to the problem was made by Schelkunoff [25]), who dealt with the case of wave guides containing media which are not only anisotropic but also inhomogeneous. As this approach is quite different from the others and ours, we shall give here a short outline of it.

In isotropic wave guides there exist two series of solutions, TM- and TE-modes, each satisfying the boundary conditions imposed by the walls. The modes possess certain orthogonality properties, and they form a complete set of solutions of Maxwell's equations. In an earlier paper Schelkunoff [24]) showed that for all isotropic wave guide modes a voltage V and a current I can be defined, which are related to the field components in a simple way, and which satisfy the telegraphist's equations

$$\mathrm{d}V/\mathrm{d}z = -ZI, \quad \mathrm{d}I/\mathrm{d}z = -YV. \tag{1.21}$$

The impedance Z and the admittance Y depend on the mode number, the electromagnetic properties of the medium and the dimensions of the wave guide. Isotropic modes are not coupled, but irregularities in the wave guide structure cause mode coupling. Now an anisotropic inhomogeneous medium can be considered as an isotropic and homogeneous medium with distributed irregularities which provide coupling between the modes of the isotropic wave guide. From the set of normal modes of the isotropic wave guide Schelkunoff derives a modified set of normal modes, and he tries to solve Maxwell's equations by a superposition of these modified normal modes. The modified normal modes are chosen in such a way that they still have the orthogonality properties of the original normal modes and that they satisfy the same boundary conditions which the original set satisfies. Then a superposition of modified normal modes satisfies automatically the boundary conditions imposed by the wall. Moreover it can be shown from Maxwell's equations that the voltages and currents connected with the modified normal modes must obey an infinite set of generalized telegraphist's equations

$$\left.\begin{aligned}
\mathrm{d}V_{m'}/\mathrm{d}z &= -\sum_{n'}(Z_{m'n'}I_{n'} + {}^{V}T_{m'n'}V_{n'}) - \sum_{n''}(Z_{m'n''}I_{n''} + {}^{V}T_{m'n''}V_{n''}),\\
\mathrm{d}I_{m'}/\mathrm{d}z &= -\sum_{n'}({}^{I}T_{m'n'}I_{n'} + Y_{m'n'}V_{n'}) - \sum_{n''}({}^{I}T_{m'n''}I_{n''} + Y_{m'n''}V_{n''}),\\
\mathrm{d}V_{m''}/\mathrm{d}z &= -\sum_{n'}(Z_{m''n'}I_{n'} + {}^{V}T_{m''n'}V_{n'}) - \sum_{n''}(Z_{m''n''}I_{n''} + {}^{V}T_{m''n''}V_{n''}),\\
\mathrm{d}I_{m''}/\mathrm{d}z &= -\sum_{n'}({}^{I}T_{m''n'}I_{n'} + Y_{m''n'}V_{n'}) - \sum_{n''}({}^{I}T_{m''n''}I_{n''} + Y_{m''n''}V_{n''}).
\end{aligned}\right\} \tag{1.22}$$

The indices m' and n' refer to modified TM-modes, the indices m'' and n'' to modified TE-modes. The impedances Z, admittances Y, and voltage- and current-transfer coefficients ${}^{V}T$, c.q. ${}^{I}T$ are very complicated integrals, but they can be evaluated, at least in principle.

The equations (22) cannot be handled in general, and Schelkunoff's method does not seem to give new practical possibilities.

Experimental work. Most of the experimental work is related to the increasingly important microwave applications of ferromagnetic ferrites. These applications are based on the fact that it is possible to change the uhf magnetic properties, and therefore the propagation constants, by applying a constant magnetic field to the ferrites. The effect which has been investigated most carefully is the Faraday rotation of waves in circular wave guides, containing ferrites that are magnetized by a constant axial magnetic field. In this case the medium becomes gyromagnetic. The effect has first been observed by Roberts [21]), but the most important contribution in this field was made by Hogan [11]) who showed that by

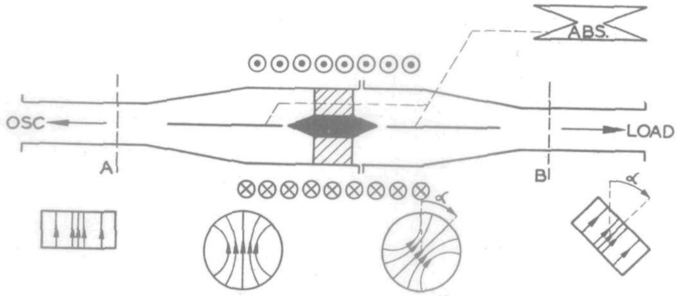

Fig. 2. Schematic drawing of a microwave Faraday rotator.

means of Faraday rotation it is possible to realize new microwave components with very desirable properties. Among these components are Tellegen's gyrator and an element which has unilateral transmission. These components are essentially new in that they violate the reciprocity relation. The same elements have been studied by Smullin [28]), by Sakiotis and Chait [23]) who investigated a large number of ferrites, and by van Trier [33]) who worked out a method for determining experimentally the elements of the scattering matrix of general passive linear microwave fourpoles. In all these experiments a Faraday rotator was used consisting of two pieces of rectangular wave guide connected by a circular wave guide in which the Faraday rotation can take place. The rectangular wave guides serve as polarizer, c.q. analyzer (fig. 2). The ferrite element is placed in the circular wave guide (when it is a needle, it is supported by a ring of foam plastic) and can be magnetized by means of a coil. The transitions from rectangular to circular cross-section are so smooth that a gradual transition from the TE_{01} rectangular mode into the TE_{11} circular mode is secured. Moreover the system contains two resistive sheets. Waves that are polarized in the plane of these sheets are largely absorbed (attenuation > 30 db), whereas waves that are polarized perpendicular to the plane of the sheets are hardly affected (attenuation < 1 db). The circular wave guide is interrupted in such a way that the analyzer can be rotated with respect to the polarizer around the axis of the system, and hence the analyzer can be adapted to the polarization of the transmitted wave.

Other investigators have applied magnetic Faraday rotation in various ways. Allen [1]) developed a microwave magnetometer using Faraday rotation as a means for measuring magnetic fields. He claims that field changes of the order of 1 gamma (10^{-5} Oe) have been detected. Olin [16]) used a Faraday rotator in the design of an X-band sweep oscillator; here the rotator was used as a modulator unit in an amplitude stabilizing feedback circuit. Finally experiments have been performed with the constant magnetic field not parallel, but perpendicular to the axis of the wave guides. It is hardly possible to analyze this system physically, but it has proved to be useful as a magnetic attenuator. Performance data of many ferrites have been published by Reggia and Beatty [20]).

Although nearly all experimental work in this field was carried out with gyromagnetic media, it must be mentioned that gyro-electric media were studied also. Goldstein, Lampert and Heney [8]) [9]) investigated guided wave propagation through gas discharges. The electron gas in the discharge becomes gyro-electric on application of a constant magnetic field. They used wave guides of both circular and rectangular cross-section. In the former large Faraday rotations were obtained.

CHAPTER II. GUIDED WAVES IN ANISOTROPIC MEDIA

In this chapter we shall study modes in wave guides containing anisotropic media. In order to obtain a general starting point we shall first consider the case of a wave guide of arbitrary cross-section filled with "Tellegen's medium". We shall derive the relations expressing the transverse in terms of the longitudinal field components and also the differential equations for the longitudinal components in Tellegen's medium with constant coefficents. From these general results we shall deduce the equations determining the fields in wave guides containing media which are both gyromagnetic and gyroelectric. We shall indicate an approach towards the general solution of Maxwell's equations under the boundary conditions imposed by the wall. Here we shall follow more or less Kales's theory. Kales, however, considered media which are gyromagnetic only, and our more general treatment includes the calculations of Suhl and Walker[29]), Gamo[7]), and Kales[13]), as well as those of Hafner[10]). In addition we shall deal with some general properties of modes in wave guides containing anisotropic media. It will be shown that no TEM-modes exist; nor do TE- or TM-modes exist except in the case of cutoff.

After these general considerations we shall work out a few examples. First of all the simplest wave guide structure will be analyzed, viz. a wave guide consisting of two parallel planes of infinite extent. As may be expected this is the structure which is most suitable for theoretical investigations, and a study of it is interesting in that it reveals many characteristics of guided waves in anisotropic media. It also gives us an opportunity to add some remarks concerning modes in wave guides of rectangular cross-section. We shall pay special attention to the transition from isotropic to anisotropic media, and we shall show, in accordance with our previous statement, that the modes in anisotropic media are no longer TM or TE. Still they may be divided into two groups, which we might call quasi-TM- and quasi-TE-modes, according to the mode type to which they reduce when the anisotropy is gradually removed.

Our second example will be the wave guide of circular cross-section. Here we shall distinguish between the cases of a completely filled wave guide and a wave guide containing a coaxial cylinder of the anisotropic medium, embedded in an isotropic medium. Some general results concerning this configuration have been obtained by Suhl and Walker, Gamo and Kales. In addition, however, we shall investigate carefully the case of partial filling with thin coaxial anisotropic cylinders.

It will turn out that these considerations suggest a method for determining the elements of the permeability tensor separately. This would admit an experimental verification of Polder's [17]) and R a-do's [19]) theories of the permeability tensor (cf. Chapter V).

§ 4. *Wave guides containing "Tellegen's medium"*. In this section we shall outline an approach towards the solution of Maxwell's equations in a wave guide containing Tellegen's medium. Describing the z-dependence of the components by the factor exp $(-\gamma z)$, they may be represented by expressions of the form $f(v_1, v_2)$ exp $(-\gamma z)$. Here $\gamma = \alpha + j\beta$, with $\alpha, \beta \geq 0$. In order to find the differential equations we write down Maxwell's equations in components (vector notation is no longer very useful in the description of fields in anisotropic media):

$$\frac{1}{h_2}\frac{\partial E_3}{\partial v_2} + \gamma E_2 = -j\omega \sum_{l=1}^{3} (\xi_{l1}^* E_l + \mu_{1l} H_l), \tag{2.1a}$$

$$-\gamma E_1 - \frac{1}{h_1}\frac{\partial E_3}{\partial v_1} = -j\omega \sum_{l=1}^{3} (\xi_{l2}^* E_l + \mu_{2l} H_l), \tag{2.1b}$$

$$\frac{1}{h_1 h_2}\left[\frac{\partial(h_2 E_2)}{\partial v_1} - \frac{\partial(h_1 E_1)}{\partial v_2}\right] = -j\omega \sum_{l=1}^{3} (\xi_{l3}^* E_l + \mu_{3l} H_l), \tag{2.1c}$$

$$\frac{1}{h_2}\frac{\partial H_3}{\partial v_2} + \gamma H_2 = j\omega \sum_{l=1}^{3} (\varepsilon_{1l} E_l + \xi_{1l} H_l), \tag{2.1d}$$

$$-\gamma H_1 - \frac{1}{h_1}\frac{\partial H_3}{\partial v_1} = j\omega \sum_{l=1}^{3} (\varepsilon_{2l} E_l + \xi_{2l} H_l), \tag{2.1e}$$

$$\frac{1}{h_1 h_2}\left[\frac{\partial(h_2 H_2)}{\partial v_1} - \frac{\partial(h_1 H_1)}{\partial v_2}\right] = j\omega \sum_{l=1}^{3} (\varepsilon_{3l} E_l + \xi_{3l} H_l). \tag{2.1f}$$

We now remark that the equations ($1a$, b, d, e) do not contain derivatives of $E_{1,2}$ and $H_{1,2}$, and that therefore we can express the transverse components in the longitudinal components and their first derivatives. Substituting these expressions into ($1c$, f) we obtain two simultaneous second order partial differential equations for E_3 and H_3. Carrying out this procedure we rewrite ($1a$, b, d, e) as

$$\left.\begin{aligned}
&j\omega\xi_{11}^* E_1 + (j\omega\xi_{21}^* + \gamma)\, E_2 + j\omega\mu_{11} H_1 + j\omega\mu_{12} H_2 = f_1(E_3, H_3),\\
&(j\omega\xi_{12}^* - \gamma) E_1 + j\omega\xi_{22}^* E_2 + j\omega\mu_{21} H_1 + j\omega\mu_{22} H_2 = f_2(E_3, H_3),\\
&j\omega\varepsilon_{11} E_1 + j\omega\varepsilon_{12} E_2 + j\omega\xi_{11} H_1 + (j\omega\xi_{12} - \gamma)\, H_2 = f_3(E_3, H_3),\\
&j\omega\varepsilon_{21} E_1 + j\omega\varepsilon_{22} E_2 + (j\omega\xi_{21} + \gamma)\, H_1 + j\omega\xi_{22} H_2 = f_4(E_3, H_3),
\end{aligned}\right\} \tag{2.2}$$

where

$$\left.\begin{aligned}
f_1 &= -\left(j\omega\xi_{31}^* + \frac{1}{h_2}\frac{\partial}{\partial v_2}\right)E_3 - j\omega\mu_{13}\,H_3,\\
f_2 &= -\left(j\omega\xi_{32}^* - \frac{1}{h_1}\frac{\partial}{\partial v_1}\right)E_3 - j\omega\mu_{23}\,H_3,\\
f_3 &= -\,j\omega\varepsilon_{13}E_3 - \left(j\omega\xi_{13} - \frac{1}{h_2}\frac{\partial}{\partial v_2}\right)H_3,\\
f_4 &= -\,j\omega\varepsilon_{23}\,E_3 - \left(j\omega\xi_{23} + \frac{1}{h_1}\frac{\partial}{\partial v_1}\right)H_3.
\end{aligned}\right\} \tag{2.3}$$

Let the determinant of the set of equations (2) be Δ, and let the minors be Δ_{kl}; then the normalized cofactors are

$$\delta_{lk} = (-)^{k+l}\,\Delta_{kl}/\Delta. \tag{2.4}$$

From (2) we find at once

$$E_1 = \sum_{k=1}^{4}\delta_{1k}f_k,\ E_2 = \sum_{k=1}^{4}\delta_{2k}f_k,\ H_1 = \sum_{k=1}^{4}\delta_{3k}f_k,\ H_2 = \sum_{k=1}^{4}\delta_{4k}\,f_k. \tag{2.5}$$

If the ε_{kl} etc. are independent of the coordinates, substitution of (5) and (2) into $(1c, f)$ yields the equations

$$\begin{aligned}
&C_1^{1,2}\frac{1}{h_1h_2}\frac{\partial}{\partial v_1}\left(\frac{h_2}{h_1}\frac{\partial E_3}{\partial v_1}\right) + C_2^{1,2}\frac{1}{h_1h_2}\frac{\partial^2 E_3}{\partial v_1\partial v_2} + C_3^{1,2}\frac{1}{h_1h_2}\frac{\partial}{\partial v_2}\left(\frac{h_1}{h_2}\frac{\partial E_3}{\partial v_2}\right)+\\
&+ C_4^{1,2}\frac{1}{h_1h_2}\frac{\partial}{\partial v_1}\left(\frac{h_2}{h_1}\frac{\partial H_3}{\partial v_1}\right)+C_5^{1,2}\frac{1}{h_1h_2}\frac{\partial^2 H_3}{\partial v_1\partial v_2}+C_6^{1,2}\frac{1}{h_1h_2}\frac{\partial}{\partial v_2}\left(\frac{h_1}{h_2}\frac{\partial H_3}{\partial v_2}\right)+\\
&+C_7^{1,2}\frac{1}{h_1h_2}\frac{\partial(h_2E_3)}{\partial v_1}+C_8^{1,2}\frac{1}{h_1h_2}\frac{\partial(h_1E_3)}{\partial v_2}+C_9^{1,2}\frac{1}{h_1}\frac{\partial E_3}{\partial v_1}+C_{10}^{1,2}\frac{1}{h_2}\frac{\partial E_3}{\partial v_2}+\\
&+C_{11}^{1,2}\frac{1}{h_1h_2}\frac{\partial(h_2H_3)}{\partial v_1}+C_{12}^{1,2}\frac{1}{h_1h_2}\frac{\partial(h_1H_3)}{\partial v_2}+C_{13}^{1,2}\frac{1}{h_1}\frac{\partial H_3}{\partial v_1}+C_{14}^{1,2}\frac{1}{h^2}\frac{\partial H_3}{\partial v_2}+\\
&+ C_{15}^{1,2}\,E_3 + C_{16}^{1,2}\,H_3 = 0.
\end{aligned} \tag{2.6}$$

These two simultaneous second order partial differential equations with constant coefficients are difficult to handle in general, but in some applications they are simplified to such an extent that an explicit solution can be given. We shall not write down the expressions for all coefficients C except for those of the second order terms. We find

$$\left.\begin{aligned}
&C_1^1=\delta_{22},\ C_2^1=-(\delta_{12}+\delta_{21}),\ C_3^1=\delta_{11},\ C_4^1=-\delta_{24},\ C_5^1=\delta_{23}+\delta_{14},\ C_6^1=-\delta_{13},\\
&C_1^2=-\delta_{42},\ C_2^2=\delta_{41}+\delta_{32},\ C_3^2=-\delta_{31},\ C_4^2=\delta_{44},\ C_5^2=-(\delta_{43}+\delta_{34}),\ C_6^2=\delta_{33}.
\end{aligned}\right\} \tag{2.7}$$

A little algebra shows that for imaginary γ

$$\delta_{11}=-\delta^*_{33},\ \delta_{22}=-\delta^*_{44},\ \delta_{12}=-\delta^*_{43},\ \delta_{21}=-\delta^*_{34},\ \delta_{14}=-\delta^*_{23},\ \delta_{41}=-\delta^*_{32}, \tag{2.8}$$

and comparison with (7) shows that for this case

$$C^1_1=-C^{2*}_4,\ C^1_2=-C^{2*}_5,\ C^1_3=-C^{2*}_6. \tag{2.9}$$

From the relations derived here one can deduce the equations determining the field in any medium without dissipation, for which the ε_{kl} are independent of the orthogonal coordinates used.

§ 5. *Wave guides containing gyromagnetic and gyroelectric media.* Let us now investigate electromagnetic fields in wave guides containing the medium defined by (1.14). Let us first evaluate some of the constants introduced in the preceding section. For Δ and the constants δ_{lk} we find

$$\Delta=\{\gamma^2+\omega^2(\varepsilon_1+\varepsilon_2)(\mu_1+\mu_2)\}\{\gamma^2+\omega^2(\varepsilon_1-\varepsilon_2)(\mu_1-\mu_2)\}, \tag{2.10}$$

$$\left.\begin{aligned}
p&=\delta_{12}=-\delta_{21}=-\delta_{34}=\delta_{43}=-\gamma[\gamma^2+\omega^2(\varepsilon_1\mu_1+\varepsilon_2\mu_2)]\,\Delta^{-1},\\
q&=-\delta_{11}=-\delta_{22}=\delta_{33}=\delta_{44}=-j\gamma\omega^2(\varepsilon_1\mu_2+\varepsilon_2\mu_1)\,\Delta^{-1},\\
r&=\delta_{23}=-\delta_{14}=\omega[\mu_2\gamma^2-\omega^2(\mu_1^2-\mu_2^2)\,\varepsilon_2]\,\Delta^{-1},\\
s&=\delta_{13}=\delta_{24}=-j\omega\,[\mu_1\gamma^2+\omega^2(\mu_1^2-\mu_2^2)\,\varepsilon_1]\,\Delta^{-1},\\
t&=\delta_{32}=-\delta_{41}=-\omega\,[\varepsilon_2\gamma^2-\omega^2(\varepsilon_1^2-\varepsilon_2^2)\,\mu_2]\,\Delta^{-1},\\
u&=-\delta_{31}=-\delta_{42}=j\omega\,[\varepsilon_1\gamma^2+\omega^2(\varepsilon_1^2-\varepsilon_2^2)\,\mu_1]\,\Delta^{-1}.
\end{aligned}\right\} \tag{2.11}$$

For the medium considered here the coefficients C in (6) have a very simple form; most of them disappear, and we only retain

$$\left.\begin{aligned}
&C^1_1=C^1_3=-C^2_4=-C^2_6=-q,\\
&C^1_4=C^1_6=-s,\ C^2_1=C^2_3=u,\ C^1_{16}=j\omega\mu_3,\ C^2_{15}=j\omega\varepsilon_3.
\end{aligned}\right\} \tag{2.12}$$

Keeping in mind that in generalized orthogonal cylindrical coordinates

$$\nabla^2\varphi\equiv\frac{1}{h_1h_2}\frac{\partial}{\partial v_1}\left(\frac{h_2}{h_1}\frac{\partial\varphi}{\partial v_1}\right)+\frac{1}{h_1h_2}\frac{\partial}{\partial v_2}\left(\frac{h_1}{h_2}\frac{\partial\varphi}{\partial v_2}\right)+\frac{\partial^2\varphi}{\partial z^2}$$

we find from (6) and (12) the equations

$$-q\nabla_t^2E_z-s\nabla_t^2H_z+j\omega\mu_3H_z=0,\quad u\nabla_t^2E_z+q\nabla_t^2H_z+j\omega\varepsilon_3E_z=0. \tag{2.13}$$

Multiplying these equations with the right factors and adding them together we can eliminate alternatively $\nabla_t^2 E_z$ and $\nabla_t^2 H_z$, obtaining thus

$$\nabla_t^2 E_z + aE_z + bH_z = 0, \quad \nabla_t^2 H_z + cH_z + dE_z = 0, \tag{2.14}$$

where

$$\left.\begin{aligned}
a &= -j\omega\varepsilon_3\, s(q^2 - su)^{-1} = (\varepsilon_3/\varepsilon_1)\,[\gamma^2 + \omega^2\varepsilon_1(\mu_1^2 - \mu_2^2)/\mu_1],\\
b &= -j\omega\mu_3\, q(q^2 - su)^{-1} = \gamma\omega\mu_3\,(\varepsilon_2/\varepsilon_1 + \mu_2/\mu_1),\\
c &= j\omega\mu_3\, u(q^2 - su)^{-1} = (\mu_3/\mu_1)\,[\gamma^2 + \omega^2\mu_1(\varepsilon_1^2 - \varepsilon_2^2)/\varepsilon_1],\\
d &= j\omega\varepsilon_3\, q(q^2 - su)^{-1} = -\gamma\omega\varepsilon_3\,(\varepsilon_2/\varepsilon_1 + \mu_2/\mu_1).
\end{aligned}\right\} \tag{2.15}$$

The relations between the transverse and the longitudinal components follow immediately from (3), (5) and (11):

$$\left.\begin{aligned}
E_1 &= p\frac{1}{h_1}\frac{\partial E_z}{\partial v_1} + q\frac{1}{h_2}\frac{\partial E_z}{\partial v_2} + r\frac{1}{h_1}\frac{\partial H_z}{\partial v_1} + s\frac{1}{h_2}\frac{\partial H_z}{\partial v_2},\\
E_2 &= -q\frac{1}{h_1}\frac{\partial E_z}{\partial v_1} + p\frac{1}{h_2}\frac{\partial E_z}{\partial v_2} - s\frac{1}{h_1}\frac{\partial H_z}{\partial v_1} + r\frac{1}{h_2}\frac{\partial H_z}{\partial v_2},\\
H_1 &= t\frac{1}{h_1}\frac{\partial E_z}{\partial v_1} + u\frac{1}{h_2}\frac{\partial E_z}{\partial v_2} + p\frac{1}{h_1}\frac{\partial H_z}{\partial v_1} + q\frac{1}{h_2}\frac{\partial H_z}{\partial v_2},\\
H_2 &= -u\frac{1}{h_1}\frac{\partial E_z}{\partial v_1} + t\frac{1}{h_2}\frac{\partial E_z}{\partial v_2} - q\frac{1}{h_1}\frac{\partial H_z}{\partial v_1} + p\frac{1}{h_1}\frac{\partial H_z}{\partial v_2}.
\end{aligned}\right\} \tag{2.16}$$

In generalized orthogonal cylindrical coordinates

$$\nabla_t\,\varphi \equiv \frac{1}{h_1}\frac{\partial\varphi}{\partial v_1}\mathbf{i}_1 + \frac{1}{h_2}\frac{\partial\varphi}{\partial v_2}\mathbf{i}_2.$$

Then (16) can be rewritten as

$$\left.\begin{aligned}
\mathbf{E}_t &= \nabla_t\,(pE_z + rH_z) - \mathbf{k}\times\nabla_t\,(qE_z + sH_z),\\
\mathbf{H}_t &= \nabla_t\,(tE_z + pH_z) - \mathbf{k}\times\nabla_t\,(uE_z + qH_z).
\end{aligned}\right\} \tag{2.17}$$

When we try to find the field in a certain configuration, our first step will be to determine the general solution of (14). Kales showed that by introducing new independent variables it is possible to derive two wave equations for these new variables which are equivalent to (14). The general solution of these equations can be found only when the method of separation of variables applies. Having found the general solution of (14) we use (17) to obtain the transverse field. The integration constants of (14) must then follow from the boundary conditions imposed by the wall of the wave guide under consideration. This boundary value problem cannot be handled except when it is possible to express the field components as products of functions depending on one coordinate only. In the remaining part of this section we shall occupy ourselves with the solution of (14), with the boundary value problem, and with some general properties of modes in anisotropic media. Before carrying out this program, however, we note that there is a large number of useful relations between the constants defined by (11) and (15); for future reference we list here some of them

$$\left.\begin{aligned} &pa + rd = -\gamma\varepsilon_3/\varepsilon_1, && qa + sd = 0, \\ &pb + rc = -\omega\mu_3\varepsilon_2/\varepsilon_1, && qb + sc = -j\omega\mu_3, \\ &pc + tb = -\gamma\mu_3/\mu_1, && qc + ub = 0, \\ &pd + ta = \omega\varepsilon_3\mu_2/\mu_1, && qd + ua = j\omega\varepsilon_3, \\ &b/d = sc/ua = (qb + sc)/(qd + ua) = -\mu_3/\varepsilon_3. && \end{aligned}\right\} \tag{2.18}$$

S o l u t i o n o f t h e e q u a t i o n s (14). These equations have been studied by K a l e s, who obtained the same set, with different constants, for a medium which is gyromagnetic only. Following K a l e s we introduce new independent variables $\varphi_{1,2}$ defined by

$$E_z = \varphi_1 + \varphi_2;\ H_z = g_1\varphi_1 + g_2\varphi_2, \tag{2.19}$$

where it is to be understood that $g_1 \neq g_2$. Substituting (19) into (14) we find

$$\left.\begin{aligned} \nabla_t^2\,\varphi_1 + (a + bg_1)\,\varphi_1 + \nabla_t^2\,\varphi_2 + (a + bg_2)\,\varphi_2 = 0, \\ g_1\,\nabla_t^2\,\varphi_1 + (d + cg_1)\,\varphi_1 + g_2\,\nabla_t^2\,\varphi_2 + (d + cg_2)\,\varphi_2 = 0. \end{aligned}\right\} \tag{2.20}$$

Suppose that it is possible to determine g_1 and g_2 such that

$$\left.\begin{aligned} a + bg_1 &= \sigma_1^2, & a + bg_2 &= \sigma_2^2, \\ d + cg_1 &= g_1\,\sigma_1^2, & d + cg_2 &= g_2\,\sigma_2^2, \end{aligned}\right\} \tag{2.21}$$

then (20) changes into

$$\left.\begin{aligned} \nabla_t^2\,\varphi_1 + \sigma_1^2\varphi_1 + \nabla_t^2\,\varphi_2 + \sigma_2^2\varphi_2 = 0, \\ g_1\,(\nabla_t^2\,\varphi_1 + \sigma_1^2\varphi_1) + g_2\,(\nabla_t^2\,\varphi_2 + \sigma_2^2\varphi_2) = 0. \end{aligned}\right\} \tag{2.22}$$

On account of the condition $g_1 \neq g_2$ it follows from (22) that φ_1 and φ_2 must satisfy the wave equations

$$\nabla_t^2\,\varphi_{1,2} + \sigma_{1,2}^2\varphi_{1,2} = 0. \tag{2.23}$$

Let us now consider $g_{1,2}$; from (21) we derive that

$$g_{1,2} = (\sigma_{1,2}^2 - a)/b = d/(\sigma_{1,2}^2 - c), \qquad (2.24)$$

and these equations show that σ_1^2 and σ_2^2 must be the roots of the quadratic equation

$$\sigma^4 - (a + c)\,\sigma^2 + ac - bd = 0. \qquad (2.25)$$

Evidently

$$\sigma_1^2 + \sigma_2^2 = a + c; \quad \sigma_1^2 - a = c - \sigma_2^2, \qquad (2.26)$$

$$\sigma_1^2\sigma_2^2 = ac - bd = (\varepsilon_3\mu_3/\varepsilon_1\mu_1)\,\Delta. \qquad (2.27)$$

Substituting a, b, c and d, as defined in (15), into (25) we find

$$\begin{aligned}\sigma_{1,2}^2 = {} & \tfrac{1}{2}[\gamma^2(\varepsilon_3/\varepsilon_1 + \mu_3/\mu_1) + \omega^2\varepsilon_3(\mu_1^2 - \mu_2^2)/\mu_1 + \omega^2\mu_3(\varepsilon_1^2 - \varepsilon_2^2)/\varepsilon_1] \pm \\ & \pm \tfrac{1}{2}\{[\gamma^2(\varepsilon_3/\varepsilon_1 - \mu_3/\mu_1) + \omega^2\varepsilon_3(\mu_1^2 - \mu_2^2)/\mu_1 - \omega^2\mu_3(\varepsilon_1^2 - \varepsilon_2^2)/\varepsilon_1]^2 - \\ & - 4\gamma^2\omega^2\varepsilon_3\mu_3(\varepsilon_2/\varepsilon_1 + \mu_2/\mu_1)^2\}^{\frac{1}{2}}. \qquad (2.28)\end{aligned}$$

As an example we shall consider a medium which is gyromagnetic only ($\varepsilon_2 = 0$), and in which $\varepsilon_3 = \varepsilon_1$, $\mu_3 = \mu_1$. Then (28) reduces to

$$\begin{aligned}\sigma_{1,2}^2 = {} & \gamma^2 + \omega^2\varepsilon_1\mu_1\,[1 - \tfrac{1}{2}(\mu_2/\mu_1)^2] \pm \\ & \pm \{(\mu_2/\mu_1)^2\,\omega^2\varepsilon_1\mu_1[-\gamma^2 + \omega^2\varepsilon_1\mu_1\,(\mu_2/2\mu_1)^2]\}^{\frac{1}{2}}. \qquad (2.29)\end{aligned}$$

It is useful to introduce reduced quantities

$$\gamma_R^2 = \gamma^2/\omega^2\varepsilon_1\mu_1, \qquad \sigma_{1,2R}^2 = \sigma_{1,2}^2/\omega^2\varepsilon_1\mu_1 \qquad (2.30)$$

which transform (29) into

$$\sigma_{1,2R}^2 = \gamma_R^2 + 1 - \tfrac{1}{2}(\mu_2/\mu_1)^2 \pm (\mu_2/\mu_1)\,[-\gamma_R^2 + (\mu_2/2\mu_1)^2]^{\frac{1}{2}}. \qquad (2.31)$$

Fig. 3 shows $\sigma_{1,2R}$ as a function of γ_R/j for the following series of values of μ_2/μ_1 : 0 ; 0.1 ; 0.3 ; 0.5. For $\gamma_R/j = 1$ we have plane wave propagation. $\gamma_R = 0$ corresponds to cutoff. From (31) it may be proved that the zeros of σ_{1R} occur for $\gamma_R/j = (1 + \mu_2/\mu_1)^{\frac{1}{2}}$, and the zeros of σ_{2R} for $\gamma_R/j = (1 - \mu_2/\mu_1)^{\frac{1}{2}}$. It will be clear that σ_{1R} is real in the interval $0 < \gamma_R/j < (1 + \mu_2/\mu_1)^{\frac{1}{2}}$, whereas σ_{2R} is real in the interval $0 < \gamma_R/j < (1 - \mu_2/\mu_1)^{\frac{1}{2}}$ and imaginary for $(1 - \mu_2/\mu_1)^{\frac{1}{2}} < < \gamma_R/j < (1 + \mu_2/\mu_1)^{\frac{1}{2}}$. The hypothetic medium, introduced here, will be used several times in the following pages to illustrate the theory.

We now return to the equations (14) and write down formally their general solution; using (24) and (26) we obtain

$$\left.\begin{aligned}E_z &= \varphi_1 + \varphi_2, \\ H_z &= b^{-1}[-a(\varphi_1 + \varphi_2) + (\sigma_1^2\varphi_1 + \sigma_2^2\varphi_2)] = \\ &= b^{-1}[c(\varphi_1 + \varphi_2) - (\sigma_2^2\varphi_1 + \sigma_1^2\varphi_2)],\end{aligned}\right\} \qquad (2.32)$$

where $\varphi_{1,2}$ are the general solutions of (23). Next we substitute (32) in (17) to find the transverse components; in doing so we use the second expression for H_z as it is particularly useful in view of the relations (18):

$$\left.\begin{aligned} \mathbf{E}_t &= b^{-1}\, \nabla_t\,[(pb + rc)\,(\varphi_1 + \varphi_2) - r(\sigma_2^2\varphi_1 + \sigma_1^2\varphi_2)] - \\ &\quad - b^{-1}\,\mathbf{k} \times \nabla_t\,[(qb + sc)\,(\varphi_1 + \varphi_2) - s(\sigma_2^2\varphi_1 + \sigma_1^2\varphi_2)], \\ \mathbf{H}_t &= b^{-1}\, \nabla_t\,[(pc + tb)\,(\varphi_1 + \varphi_2) - p(\sigma_2^2\varphi_1 + \sigma_1^2\varphi_2)] - \\ &\quad - b^{-1}\,\mathbf{k} \times \nabla_t\,[(qc + ub)\,(\varphi_1 + \varphi_2) - q(\sigma_2^2\varphi_1 + \sigma_1^2\varphi_2)]. \end{aligned}\right\} \quad (2.33)$$

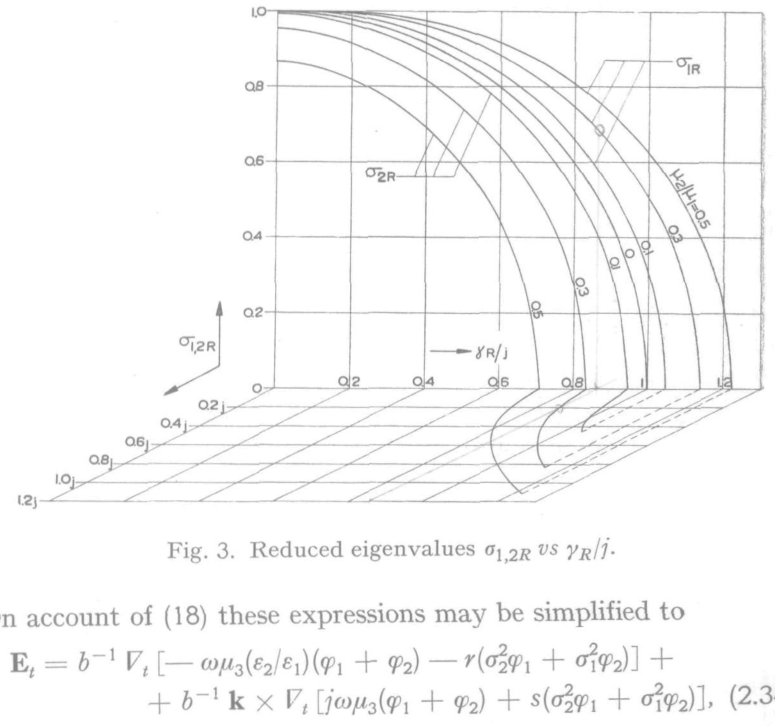

Fig. 3. Reduced eigenvalues $\sigma_{1,2R}$ *vs* γ_R/j.

On account of (18) these expressions may be simplified to

$$\begin{aligned} \mathbf{E}_t &= b^{-1}\, \nabla_t\,[-\,\omega\mu_3(\varepsilon_2/\varepsilon_1)(\varphi_1 + \varphi_2) - r(\sigma_2^2\varphi_1 + \sigma_1^2\varphi_2)] + \\ &\quad + b^{-1}\,\mathbf{k} \times \nabla_t\,[j\omega\mu_3(\varphi_1 + \varphi_2) + s(\sigma_2^2\varphi_1 + \sigma_1^2\varphi_2)], \end{aligned} \quad (2.34)$$

$$\begin{aligned} \mathbf{H}_t &= b^{-1}\, \nabla_t\,[-\,\gamma(\mu_3/\mu_1)(\varphi_1 + \varphi_2) - p(\sigma_2^2\varphi_1 + \sigma_1^2\varphi_2)] + \\ &\quad + b^{-1}\,\mathbf{k} \times \nabla_t\,[q(\sigma_2^2\varphi_1 + \sigma_1^2\varphi_2)]. \end{aligned} \quad (2.35)$$

The boundary value problem. Our next problem is to determine the integration constants in $\varphi_{1,2}$ with the help of the boundary conditions imposed by the wall. The boundary conditions require that at every point P at the wall (see fig. 4)

$$E_z = E_\tau = B_\nu = 0, \qquad (2.36)$$

where $\boldsymbol{\tau}$ and $\boldsymbol{\nu}$ are tangential and normal unit vectors. We may omit the condition $B_\nu = 0$ as it is not independent of the other two conditions; this is an immediate consequence of Maxwell's equations. We know E_z from (32), and E_τ can be found from (34):

$$E_\tau = b^{-1}\left[-\omega\mu_3 \frac{\varepsilon_2}{\varepsilon_1}\frac{\partial}{\partial\tau}(\varphi_1+\varphi_2) - r\frac{\partial}{\partial\tau}(\sigma_2^2\varphi_1+\sigma_1^2\varphi_2) + \right.$$
$$\left. + j\omega\mu_3\frac{\partial}{\partial\nu}(\varphi_1+\varphi_2) + s\frac{\partial}{\partial\nu}(\sigma_2^2\varphi_1+\sigma_1^2\varphi_2)\right]. \qquad (2.37)$$

So we find the boundary conditions at the wall in the rather simple form mag niet weggelaten worden.

$$\left.\begin{aligned} &\varphi_1+\varphi_2 = 0,\\ &r\frac{\partial}{\partial\tau}(\sigma_2^2\varphi_1+\sigma_1^2\varphi_2) - s\frac{\partial}{\partial\nu}(\sigma_2^2\varphi_1+\sigma_1^2\varphi_2) - j\omega\mu_3\frac{\partial}{\partial\nu}(\varphi_1+\varphi_2)=0.\end{aligned}\right\} \qquad (2.38)$$

The first term on the right hand side of (37) has been omitted since, when $\varphi_1+\varphi_2 = 0$ at the wall (first boundary condition), also $\partial(\varphi_1+\varphi_2)/\partial\tau = 0$. In the next sections (38) will be applied to several configurations.

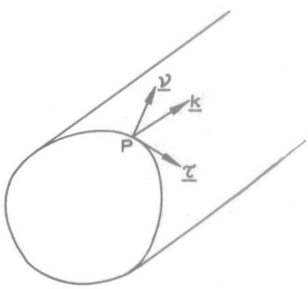

Fig. 4. Definition of tangential and normal unit vectors.

S o m e c h a r a c t e r i s t i c s o f w a v e g u i d e m o d e s i n a n i s o t r o p i c m e d i a. From (14) we may conclude that if $E_z = 0$, also $H_z = 0$, and if $H_z = 0$, also $E_z = 0$. This means that no TM- or TE-modes exist in general. The only exception occurs if $b = d = 0$. In a gyromedium (with either μ_2, or ε_2, or both $\neq 0$) b and d disappear only when $\gamma = 0$, i.e. at cutoff. For $\gamma = 0$ we find from (14) and (15):

$$\nabla_t^2 E_z + a_c E_z = 0, \quad \nabla_t^2 H_z + c_c H_z = 0, \qquad (2.39)$$
$$a_c = \omega^2\varepsilon_3(\mu_1^2-\mu_2^2)/\mu_1, \quad c_c = \omega^2\mu_3(\varepsilon_1^2-\varepsilon_2^2)/\varepsilon_1. \qquad (2.40)$$

The transverse field is obtained from (17), where $p = q = 0$.

$$\mathbf{E}_t = r\, \nabla_t H_z - s\, \mathbf{k} \times \nabla_t H_z, \quad \mathbf{H}_t = t\, \nabla_t E_z - u\, \mathbf{k} \times \nabla_t E_z. \tag{2.41}$$

Thus we see that the cutoff-fields are indeed TM or TE. Denoting the eigenvalues of a_c and c_c by $\beta'^2_{cn} = (2\pi/\lambda'_{cn})^2$ and $\beta''^2_{cn} = (2\pi/\lambda''_{cn})^2$ we find as cutoff-frequencies for the different modes

$$\omega'_{cn} = \beta'_{cn}\, [\varepsilon_3(\mu_1^2 - \mu_2^2)/\mu_1]^{-\frac{1}{2}}, \quad \omega''_{cn} = \beta''_{cn}\, [\mu_3(\varepsilon_1^2 - \varepsilon_2^2)/\varepsilon_1]^{-\frac{1}{2}}. \tag{2.42}$$

Next we may ask if TEM-modes can exist in wave guides containing gyro-media, i.e. modes in which $E_z = H_z = 0$. From (17) we see that if $E_z = H_z = 0$, also $\mathbf{E}_t = \mathbf{H}_t = 0$ unless one or more of the coefficients p, q, r, s, t, u become infinite. These coefficients, according to (11), have the common denominator Δ, which becomes zero if

$$\gamma^2 = -\omega^2(\varepsilon_1 + \varepsilon_2)(\mu_1 + \mu_2) \text{ or } \gamma^2 = -\omega^2(\varepsilon_1 - \varepsilon_2)(\mu_1 - \mu_2). \tag{2.43}$$

In order to prove that no TEM-modes can exist it is most convenient to start from Maxwell's equations (1.1); separating in these equations transverse and longitudinal components, and substituting $E_z = H_z = 0$, we find for a medium which is both gyromagnetic and gyroelectric

$$\begin{aligned} \nabla_t \times \mathbf{E}_t - \gamma\, \mathbf{k} \times \mathbf{E}_t &= -j\omega\mu_1\, \mathbf{H}_t + \omega\mu_2\, \mathbf{k} \times \mathbf{H}_t, \\ \nabla_t \times \mathbf{H}_t - \gamma\, \mathbf{k} \times \mathbf{H}_t &= j\omega\varepsilon_1\, \mathbf{E}_t - \omega\varepsilon_2\, \mathbf{k} \times \mathbf{E}_t. \end{aligned} \tag{2.44}$$

Equating transverse and longitudinal components we obtain

$$\nabla_t \times \mathbf{E}_t = 0, \quad \nabla_t \times \mathbf{H}_t = 0, \tag{2.45a}$$

$$-\gamma\, \mathbf{k} \times \mathbf{E}_t + j\omega\mu_1\, \mathbf{H}_t - \omega\mu_2\, \mathbf{k} \times \mathbf{H}_t = 0, \tag{2.45b}$$

$$-\gamma\, \mathbf{k} \times \mathbf{H}_t - j\omega\varepsilon_1\, \mathbf{E}_t + \omega\varepsilon_2\, \mathbf{k} \times \mathbf{E}_t = 0. \tag{2.45c}$$

From (45c) we derive

$$\mathbf{k} \times \mathbf{H}_t = \gamma^{-1}\, [-j\omega\varepsilon_1\, \mathbf{E}_t + \omega\varepsilon_2\, \mathbf{k} \times \mathbf{E}_t], \tag{2.46a}$$

and multiplying vectorially by $\mathbf{k}$

$$\mathbf{H}_t = \gamma^{-1}\, [j\omega\varepsilon_1\, \mathbf{k} \times \mathbf{E}_t + \omega\varepsilon_2\, \mathbf{E}_t]. \tag{2.46b}$$

Substitution of (46) in (45b) leads to

$$[\gamma^2 + \omega^2(\varepsilon_1\mu_1 + \varepsilon_2\mu_2)]\, \mathbf{k} \times \mathbf{E}_t - j\omega^2(\varepsilon_1\mu_2 + \varepsilon_2\mu_1)\, \mathbf{E}_t = 0, \tag{2.47}$$

and in view of (43) this reduces to

$$\mathbf{k} \times \mathbf{E}_t \pm j\mathbf{E}_t = 0. \tag{2.48}$$

Suppose

$$\left.\begin{aligned} \mathbf{E}_t &= E_1\,\mathbf{i}_1 \exp j\psi_1 + E_2\,\mathbf{i}_2 \exp j\psi_2, \\ \mathbf{k}\times\mathbf{E}_t &= -\,E_2\,\mathbf{i}_1 \exp j\psi_2 + E_1\,\mathbf{i}_2 \exp j\psi_1, \end{aligned}\right\} \quad (2.49)$$

Substituting this into (48) we find

$$E_2 = E_1, \qquad \psi_2 = \psi_1 \pm \pi/2. \qquad (2.50)$$

This means that a TEM-mode, if it exists, is right or left circularly polarized. Let us now consider a wave guide of arbitrary cross-section which may be multiply connected. The boundary condition for the electric field requires that the tangential component of $\mathbf{E}_t$ disappears at the walls, but on account of (50) the normal component then disappears also, i.e. $\mathbf{E}_t = 0$ at the walls. Because of (46*b*) also $\mathbf{H}_t = 0$ at the walls. But if the field vanishes at the wave guide walls, it can be shown to vanish everywhere within the wave guide. Therefore no TEM-mode exists in a wave guide containing anisotropic media.

§ 6. *Wave guides consisting of two parallel planes.* As a first application we shall investigate the simplest wave guide structure, viz. a

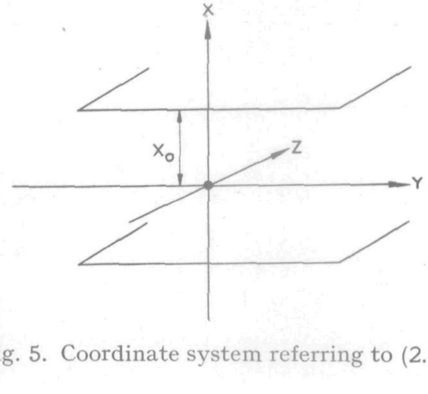

Fig. 5. Coordinate system referring to (2.51).

wave guide consisting of two parallel planes of infinite extent. It will be of interest to study the relations between modes in anisotropic media and modes in isotropic media. Therefore we give here, without proof, the expressions describing the modes in isotropic media. Let the two parallel planes be $x = \pm\, x_0$ (see fig. 5). Then the fields with z-dependence exp $(-\,\gamma z)$ have the following form:

propagation parallel to gyroaxis!

$$\left.\begin{aligned}
&\text{In TM}_n\text{-modes } (n = 0, 1, 2, 3, \ldots)\\
&E_x = \hat{E}_x\,[\exp\,(j\sigma_{0n}\,x) + (-)^n \exp\,(-\,j\sigma_{0n}\,x)]\,\exp\,(-\,\gamma_{0n}\,z),\\
&H_y = (j\omega\varepsilon/\gamma_{0n})\hat{E}_x\,[\exp(j\sigma_{0n}x) + (-)^n \exp(-j\sigma_{0n}x)]\,\exp(-\gamma_{0n}z),\\
&E_z = (j\sigma_{0n}/\gamma_{0n})\hat{E}_x[\exp(j\sigma_{0n}\,x) - (-)^n \exp(-j\sigma_{0n}\,x)]\exp(-\gamma_{0n}z).\\
&\text{In TE}_n\text{-modes } (n = 1, 2, 3 \ldots)\\
&E_y = \hat{E}_y\,[\exp\,(j\sigma_{0n}\,x) - (-)^n \exp\,(-\,j\sigma_{0n}\,x)]\,\exp\,(-\,\gamma_{0n}\,z),\\
&H_x = -(\gamma_{0n}/j\omega\mu)\hat{E}_y[\exp(j\sigma_{0n}x) - (-)^n\exp(-j\sigma_{0n}x)]\exp(-\gamma_{0n}z),\\
&H_z = -(\sigma_{0n}/\omega\mu)\hat{E}_y[\exp(j\sigma_{0n}x) + (-)^n\exp(-j\sigma_{0n}x)]\exp(-\gamma_{0n}z).
\end{aligned}\right\} \quad (2.51)$$

For both mode types

$$\gamma_{0n}^2 = -\,\omega^2\varepsilon\mu + (n\pi/2x_0)^2 = -\,\omega^2\varepsilon\mu + \sigma_{0n}^2. \quad (2.52)$$

These γ's and σ's have been provided with an additional subscript 0 to distinguish them from the γ's and σ's which we shall find in the anisotropic media. The TM_0-mode is TEM; the TE_0-mode does not exist, as one sees at once on substituting $n = 0$ into (51).

Next we assume the space between the plates to be filled with the medium (1.14). We can simply apply the general results of the preceding section. The equations (23) for $\varphi_{1,2}$ reduce to

$$(\mathrm{d}^2/\mathrm{d}x^2 + \sigma_{1,2}^2)\,\varphi_{1,2} = 0, \quad (2.53)$$

for $\partial/\partial y \equiv 0$, as the field components are independent of y. The general solutions of (53) are

$$\left.\begin{aligned}
\varphi_1 &= A_1'[\exp(j\sigma_1 x) + \exp(-j\sigma_1 x)] + A_1''[\exp(j\sigma_1 x) - \exp(-j\sigma_1 x)],\\
\varphi_2 &= A_2'[\exp(j\sigma_2 x) + \exp(-j\sigma_2 x)] + A_2''[\exp(j\sigma_2 x) - \exp(-j\sigma_2 x)].
\end{aligned}\right\} \quad (2.54)$$

In these solutions we have separated symmetrical and antisymmetrical terms as we shall try to solve the boundary value problem with symmetrical, c.q. antisymmetrical $\varphi_{1,2}$ only. The boundary conditions which determine the values of the propagation constants can be derived from (38). Noting that in the present configuration at the plates $x = \pm\, x_0$: $\partial/\partial \nu = \pm\, \partial/\partial x$; $\partial/\partial\tau = \pm\,\partial/\partial y \equiv 0$, we find the boundary conditions for $x = \pm\, x_0$:

$$\varphi_1 + \varphi_2 = 0, \frac{\partial}{\partial x}\,[(s\sigma_2^2 + j\omega\mu_3)\,\varphi_1 + (s\sigma_1^2 + j\omega\mu_3)\,\varphi_2] = 0. \quad (2.55)$$

Substituting the symmetrical $\varphi_{1,2}$, represented by the A'-terms in (54), into (55) we get

$$\left.\begin{aligned} &A_1' [\exp (j\sigma_1 x_0) + \exp(-j\sigma_1 x_0)] + \\ &\qquad + A_2' [\exp (j\sigma_2 x_0) + \exp (-j\sigma_2 x_0)] = 0, \\ &j\sigma_1 A_1'(s\sigma_2^2 + j\omega\mu_3) [\exp (j\sigma_1 x_0) - \exp (-j\sigma_1 x_0)] + \\ &\quad + j\sigma_2 A_2' (s\sigma_1^2 + j\omega\mu_3) [\exp (j\sigma_2 x_0) - \exp (-j\sigma_2 x_0)] = 0. \end{aligned}\right\} \quad (2.56)$$

As is well-known, it follows from a set of equations like (56) that $A_1' = A_2' = 0$ unless the determinant vanishes; this furnishes us with the relation

$$\begin{aligned} &\sigma_2(s\sigma_1^2 + j\omega\mu_3) [\exp (j\sigma_1 x_0) + \exp (-j\sigma_1 x_0)] \cdot \\ &\qquad\qquad . [\exp (j\sigma_2 x_0) - \exp (-j\sigma_2 x_0)] - \\ &\qquad - \sigma_1(s\sigma_2^2 + j\omega\mu_3) [\exp (j\sigma_1 x_0) - \exp (-j\sigma_1 x_0)] \cdot \\ &\qquad\qquad . [\exp (j\sigma_2 x_0) + \exp (-j\sigma_2 x_0)] = 0. \quad (2.57) \end{aligned}$$

Starting from the antisymmetrical $\varphi_{1,2}$, the A''-terms in (54), we can derive in the same way the equation

$$\begin{aligned} &\sigma_2(s\sigma_1^2 + j\omega\mu_3) [\exp (j\sigma_1 x_0) - \exp (-j\sigma_1 x_0)] \cdot \\ &\qquad\qquad . [\exp (j\sigma_2 x_0) + \exp (-j\sigma_2 x_0)] - \\ &\qquad - \sigma_1(s\sigma_2^2 + j\omega\mu_3) [\exp (j\sigma_1 x_0) + \exp (-j\sigma_1 x_0)] \cdot \\ &\qquad\qquad . [\exp (j\sigma_2 x_0) - \exp (-j\sigma_2 x_0)] = 0. \quad (2.58) \end{aligned}$$

When the frequency, the electromagnetic constants of the medium and the plate distance are given, (57) and (58) may be considered as the characteristic equations whose roots determine the propagation constants of guided waves between the plates. The characteristic equations are transcendental and must be solved by graphical methods.

We shall now work out an example which will reveal many characteristics of guided waves in anisotropic media. We consider the same media that have been introduced in the preceding section, and for which we know $\sigma_{1,2R}$ (see fig. 3). Substituting s from (11) and introducing reduced quantities again, we find easily

$$\begin{aligned} s\sigma_{1,2}^2 &= \frac{-j\omega\mu_1 [\gamma^2 + \omega^2\varepsilon\mu_1 - \omega^2\varepsilon\mu_1 (\mu_2/\mu_1)^2]}{(\gamma^2 + \omega^2\varepsilon\mu_1)^2 - \omega^4\varepsilon^2\mu_1^2 (\mu_2/\mu_1)^2} \sigma_{1,2}^2 = \\ &= -j\omega\mu_1 \frac{\gamma_R^2 + 1 - (\mu_2/\mu_1)^2}{(\gamma_R^2 + 1)^2 - (\mu_2/\mu_1)^2} \sigma_{1,2R}^2 = -j\omega\mu_1 U\sigma_{1,2R}^2, \quad (2.59) \end{aligned}$$

where

$$U = [\gamma_R^2 + 1 - (\mu_2/\mu_1)^2]\Big/[(\gamma_R^2 + 1)^2 - (\mu_2/\mu_1)^2]. \qquad (2.60)$$

In order to obtain an abbreviated notation for (57) and (58) we define quantities $O_{1,2}$ and $P_{1,2}$ as

$$\left.\begin{aligned} O_{1,2} &= \sigma_{2,1R}(1 - U\sigma_{1,2R}^2), \\ P_{1,2} &= (1/4j)\,[\exp\,(j\sigma_{1,2R}x_{0R}) + \exp\,(-j\sigma_{1,2R}x_{0R})]\,\cdot \\ &\quad \cdot\,[\exp\,(j\sigma_{2,1R}x_{0R}) - \exp\,(-j\sigma_{2,1R}x_{0R})]. \end{aligned}\right\} \qquad (2.61)$$

Here we have introduced a reduced plate distance $x_{0R} = x_0(\omega^2\varepsilon\mu_1)^{\frac{1}{2}}$. On account of the fact that in our hypothetic medium $\mu_3 = \mu_1$, (57) and (58) are equivalent to

$$M_1 = O_1P_1 - O_2P_2 = 0, \qquad M_2 = O_1P_2 - O_2P_1 = 0. \quad (2.62)$$

In fig. 6 we have plotted $|M_1|^{\frac{1}{2}}$ and $|M_2|^{\frac{1}{2}}$ against γ_R/j for $x_{0R} = 5$. The zero's of $M_{1,2}$ determine the propagation constants of the modes which are propagated without attenuation.

Several remarks can be made concerning these graphs. First of all we notice that $U \to \infty$ if $\gamma_R^2 + 1 \to \mp\,\mu_2/\mu_1$. Comparison with (31) shows that these points coincide with the zero's of σ_{1R} and σ_{2R}. We are then able to sketch the behaviour of M_1 and M_2 as a function of γ_R/j. In the interval $0 < \gamma_R/j < (1 - \mu_2/\mu_1)^{\frac{1}{2}}$ both σ_{1R} and σ_{2R} are real; then M_1 and M_2 are also real. In the interval $(1 - \mu_2/\mu_1)^{\frac{1}{2}} < < \gamma_R/j < (1 + \mu_2/\mu_1)^{\frac{1}{2}}$ only σ_{1R} is real; σ_{2R} is positive imaginary, and this results in a real M_1 and an imaginary M_2. At the points $\gamma_R/j = (1 \pm \mu_2/\mu_1)^{\frac{1}{2}}$ there are singularities in M_2: $|M_2| \to \infty$, whereas $|M_1|$ remains finite. This is illustrated in fig. 6.

It is to be expected that the modes corresponding to the values of γ_R which we have found from $M_{1,2} = 0$ will transform into the TM_n- and TE_n-modes of (51) when we let $\mu_2/\mu_1 \to 0$. We shall now investigate this transition. It is clear that for $\mu_2/\mu_1 \to 0$ the roots of (62) and the values of $\sigma_{1,2R}$ connected with them will approach γ_{0nR} and σ_{0nR}, where

$$\gamma_{0nR}^2 = -1 + \sigma_{0nR}^2, \quad \sigma_{0nR} = n\pi/2x_{0R}. \qquad (2.63)$$

(63) is the reduced form of (52). Using (32), (34) and (35) we obtain

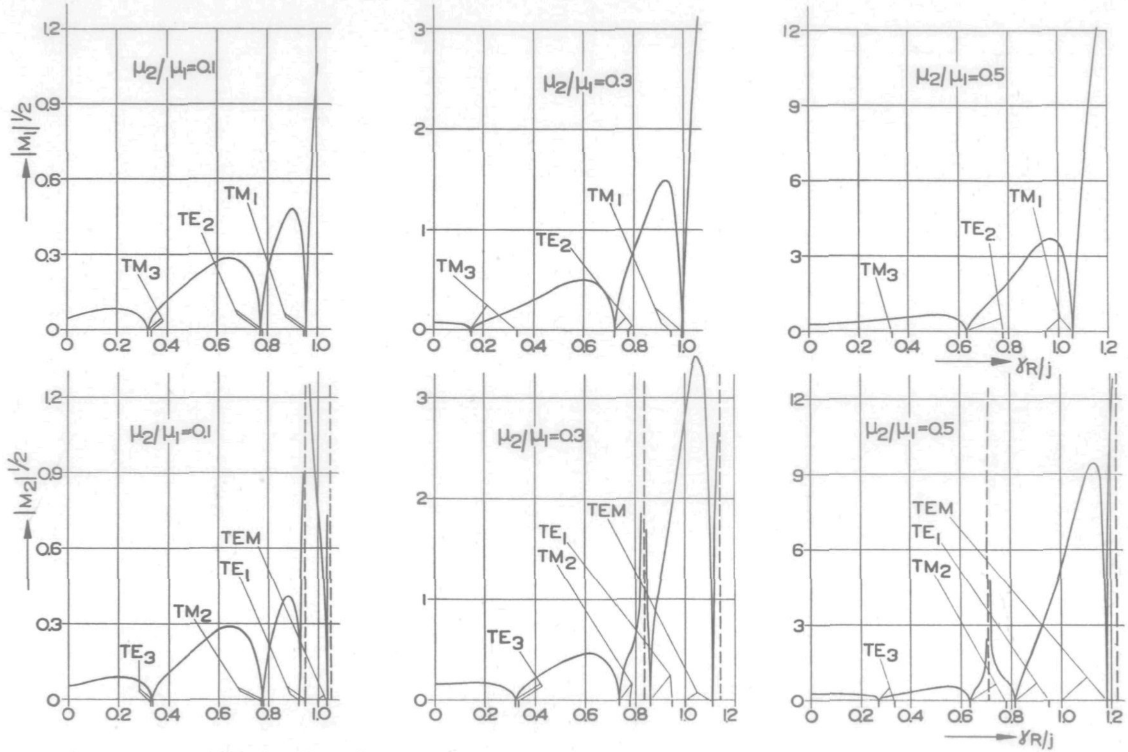

Fig. 6. $|M_{1,2}|^{\frac{1}{2}}$ *vs* γ_R/j for various values of the parameter μ_2/μ_1.

the expressions for the field components

$$\left.\begin{aligned}
&E_z = \varphi_1 + \varphi_2, \quad H_z = b^{-1}\,[(\sigma_1^2 - a)\,\varphi_1 + (\sigma_2^2 - a)\,\varphi_2],\\
&E_x = -\,b^{-1}\,r\,\frac{\partial}{\partial x}\,(\sigma_2^2\varphi_1 + \sigma_1^2\varphi_2),\\
&E_y = b^{-1}\left[(j\omega\mu_1 + s\sigma_2^2)\,\frac{\partial\varphi_1}{\partial x} + (j\omega\mu_1 + s\sigma_1^2)\,\frac{\partial\varphi_2}{\partial x}\right],\\
&H_x = -\,b^{-1}\left[(\gamma + p\sigma_2^2)\,\frac{\partial\varphi_1}{\partial x} + (\gamma + p\sigma_1^2)\,\frac{\partial\varphi_2}{\partial x}\right],\\
&H_y = b^{-1}\,q\,\frac{\partial}{\partial x}\,(\sigma_2^2\,\varphi_1 + \sigma_1^2\,\varphi_2).
\end{aligned}\right\} \tag{2.64}$$

It is easily verified that

$$\left.\begin{aligned}
&\lim_{\mu_2/\mu_1\to 0} \sigma_2^2/\sigma_1^2 = 1, \qquad \lim_{\mu_2/\mu_1\to 0} (j\omega\mu_1 + s\sigma_1^2)/(j\omega\mu_1 + s\sigma_2^2) = -\,1,\\
&\lim_{\mu_2/\mu_1\to 0} (\gamma + p\sigma_2^2)/(\gamma + p\sigma_1^2) = -\,1, \ \lim_{\mu_2/\mu_1\to 0} (\sigma_1^2 - a)/(\sigma_2^2 - a) = -\,1.
\end{aligned}\right\} \tag{2.65}$$

Moreover the limits of $b^{-1}(\sigma_{1,2}^2 - a)$, $b^{-1}(j\omega\mu_1 + s\sigma_{1,2}^2)$, $b^{-1}(\gamma + p\sigma_{1,2}^2)$, $b^{-1}r$ and $b^{-1}q$ are finite. From (65) and (55), we conclude that in the limit the boundary conditions approach to

$$\varphi_1 + \varphi_2 = 0, \tag{2.66a}$$

$$\partial(\varphi_1 - \varphi_2)/\partial x = 0. \tag{2.66b}$$

Let us first investigate the roots of $M_1 = 0$; we substitute the symmetrical part of $\varphi_{1,2}$ of (54) in (66), keeping in mind that in the limit $\sigma_{1n} = \sigma_{2n} = \sigma_{0n} = n\pi/2x_0$. We must distinguish between the cases n even and n odd:

a) n odd. In this case $(\varphi_{1,2})_{x=\pm x_0} = 0$, whereas $(\partial\varphi_1/\partial x)_{x=x_0} = 2j\sigma_{0n}\,A_1'$ and $(\partial\varphi_2/\partial x)_{x=x_0} = 2j\sigma_{0n}\,A_2'$. On account of (66*b*) we then have in the limit $A_1' = A_2'$, and $\varphi_1 = \varphi_2$. Substituting these results into (64) and using (65) we conclude that for n odd in the limit $\mu_2/\mu_1 \to 0$ the components E_y, H_x and $H_z \to 0$, whereas E_x, E_z and H_y remain finite. Comparison with (51) shows that in the limit the fields become TM_n-modes.

b) n even. Now $(\varphi_1)_{x=x_0} = 2A_1'$, $(\varphi_2)_{x=x_0} = 2A_2'$; $(\partial\varphi_{1,2}/\partial \mathrm{x})_{x=\pm x_0} = 0$. Because of (66*a*) $A_1' = -\,A_2'$, $\varphi_1 = -\,\varphi_2$. Here the components E_x, E_z and $H_y \to 0$, whereas E_y, H_x and H_z remain finite. So in the limit these fields become TE_n-modes.

Thus we see that the roots of $M_1 = 0$ determine the propagation constants of quasi-TM$_n$-modes for n odd, and quasi-TE$_n$-modes for n even. In a similar way it may be shown that the roots of $M_2 = 0$ correspond to quasi-TE$_n$-modes for n odd and to quasi-TM$_n$-modes for n even. In fig. 7 the field distributions of the TM$_1$- and the quasi-TM$_1$-modes have been drawn. Table I contains the reduced propagation constants γ_R of the different modes as derived from our graph, c.q. from an approximation which will be dealt with shortly.

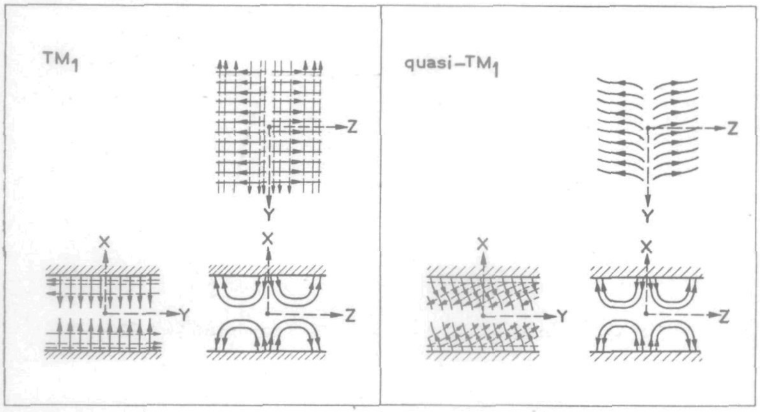

Fig. 7. Qualitative field distributions in the TM$_1$- and in the quasi-TM$_1$-mode.

TABLE I

mode	$\|\gamma_{0nR}\|$	$\|\gamma_{nR}\|_{\mu_2/\mu_1=0.1}$ graph	$\|\gamma_{nR}\|_{\mu_2/\mu_1=0.1}$ approx.	$\|\gamma_{nR}\|_{\mu_2/\mu_1=0.3}$ graph	$\|\gamma_{nR}\|_{\mu_2/\mu_1=0.3}$ approx.	$\|\gamma_{nR}\|_{\mu_2/\mu_1=0.5}$ graph	$\|\gamma_{nR}\|_{\mu_2/\mu_1=0.5}$ approx.
TEM	1.000	1.04	—	1.11	—	1.185	—
TM$_1$	0.949	0.955	0.956	0.995	1.009	1.055	1.12
TM$_2$	0.778	0.773	0.774	0.734	0.742	0.64	0.68
TM$_3$	0.334	0.320	0.320	0.15	0.204	—	—
TE$_1$	0.949	0.922	0.913	0.86	0.62	0.815	0.05
TE$_2$	0.778	0.770	0.771	0.722	0.714	0.63	0.600
TE$_3$	0.334	0.333	0.333	0.320	0.321	0.275	0.299

It is interesting to note that for all TE-modes γ_R decreases when the anisotropy increases. The same applies to the TM$_2$- and the TM$_3$-mode, but the opposite is true for the TM$_1$- and the TEM-mode. The explanation of this peculiarity will be given below.

Now that we have solved (62) for the special configuration considered here, and that we have identified the various modes as quasi-

TM and quasi-TE, we finally find a first order approximation for the roots of (62) when $\mu_2/\mu_1 \ll 1$. We develop $\sigma_{1,2R}$ and γ_R into power series of μ_2/μ_1 and we neglect all powers higher than the second:

$$\left.\begin{aligned}
\sigma_{1nR} &= \sigma_{0nR} + \varDelta\sigma_{1nR} = \sigma_{0nR}\,[1 + a_1(\mu_2/\mu_1) + a_2(\mu_2/\mu_1)^2],\\
\sigma_{2nR} &= \sigma_{0nR} - \varDelta\sigma_{2nR} = \sigma_{0nR}\,[1 - b_1(\mu_2/\mu_1) - b_2(\mu_2/\mu_1)^2],\\
\gamma_{nR} &= \gamma_{0nR} + \varDelta\gamma_{nR} = \gamma_{0nR}\,[1 + c_1(\mu_2/\mu_1) + c_2(\mu_2/\mu_1)^2].
\end{aligned}\right\} \quad (2.67a)$$

Substituting these expressions into (31) we may derive

$$\left.\begin{aligned}
&a_1 = (\gamma_{0R}^2/\sigma_{0R}^2)\,c_1 + \gamma_{0R}/2j\sigma_{0R}^2, \quad b_1 = -(\gamma_{0R}^2/\sigma_{0R}^2)\,c_1 + \gamma_{0R}/2j\sigma_{0R}^2,\\
&a_2 = (\gamma_{0R}^2/2\sigma_{0R}^4)c_1^2 + (\gamma_{0R}/2j\sigma_{0R}^4)c_1 + (\gamma_{0R}^2/\sigma_{0R}^2)c_2 + \gamma_{0R}^2/8\sigma_{0R}^4 - 1/4\sigma_{0R}^2,\\
&b_2 = -(\gamma_{0R}^2/2\sigma_{0R}^4)c_1^2 + (\gamma_{0R}/2j\sigma_{0R}^4)\,c_1 - (\gamma_{0R}^2/\sigma_{0R}^2)c_2 - \gamma_{0R}^2/8\sigma_{0R}^4 + 1/4\sigma_{0R}^2.
\end{aligned}\right\} \quad (2.67b)$$

It can also be derived that

$$\left.\begin{aligned}
&[(\gamma_R^2 + 1)^2 - (\mu_2/\mu_1)^2]\,(1 - U\sigma_{1R}^2) = j\gamma_{0R}\,\sigma_{0R}^2\,(\mu_2/\mu_1) +\\
&\qquad + (\gamma_{0R}^2 + \tfrac{1}{2}\sigma_{0R}^2)\,(1 - 2c_1\gamma_{0R}/j)\,(\mu_2/\mu_1)^2,\\
&[(\gamma_R^2 + 1)^2 - (\mu_2/\mu_1)^2]\,(1 - U\sigma_{2R}^2) = -j\gamma_{0R}\sigma_{0R}^2(\mu_2/\mu_1) +\\
&\qquad + (\gamma_{0R}^2 + \tfrac{1}{2}\sigma_{0R}^2)\,(1 + 2c_1\,\gamma_{0R}/j)\,(\mu_2/\mu_1)^2.
\end{aligned}\right\} \quad (2.68)$$

Moreover we have for n odd

$$\left.\begin{aligned}
P_1 &= -\sigma_{0R}x_{0R}\,[a_1(\mu_2/\mu_1) + a_2(\mu_2/\mu_1)^2],\\
P_2 &= \sigma_{0R}\,x_{0R}\,[b_1(\mu_2/\mu_1) + b_2(\mu_2/\mu_1)^2]
\end{aligned}\right\} \quad (2.69a)$$

and for n even

$$\left.\begin{aligned}
P_1 &= -\sigma_{0R}\,x_{0R}\,[b_1(\mu_2/\mu_1) + b_2(\mu_2/\mu_1)^2],\\
P_2 &= \sigma_{0R}\,x_{0R}\,[a_1(\mu_2/\mu_1) + a_2(\mu_2/\mu_1)^2].
\end{aligned}\right\} \quad (2.69b)$$

Substituting all this into (6~~7~~2) we find for all cases

$$c_1 = 0. \quad (2.70)$$

From $M_1 = 0$ we find for n odd

$$c_2 = (5\sigma_{0R}^2 - 1)/8\gamma_{0R}^2\,\sigma_{0R}^2 \quad (2.71)$$

and for n even

$$c_2 = -3/8\sigma_{0R}^2. \quad (2.72)$$

From $M_2 = 0$, however, we find for n odd: (7~~7~~2), and for n even: (7~~6~~1). In view of what we have seen above about the TM- or TE-character of the modes connected with the different roots of

$M_{1,2} = 0$, we may conclude that for quasi-TM_n-modes (all n)

$$\Delta\gamma_R/j = -\tfrac{1}{2}(\gamma_{0R}/j)^{-1}\,[(5\sigma_{0R}^2 - 1)/4\sigma_{0R}^2]\,(\mu_2/\mu_1)^2, \tag{2.73}$$

and for quasi-TE_n-modes (all n)

$$\Delta\gamma_R/j = -(\gamma_{0R}/j)\,(3/8\sigma_{0R}^2)\,(\mu_2/\mu_1)^2. \tag{2.74}$$

In table I we have given approximate γ_R/j-values, computed from (78) and (79). Comparison with the values which have been determined graphically shows that there is good agreement for $\mu_2/\mu_1 = 0.1$ and fair agreement for $\mu_2/\mu_1 = 0.3$; 0.5. Only for the TE_1-mode very large discrepancies occur; here the correction is much too large even for $\mu_2/\mu_1 = 0.1$. From (79) we see that $\Delta\gamma_R/j$ is negative for all TE-modes, in accordance with our previous observation. For the TM-modes the situation is different; here the sign of $\Delta\gamma_R/j$ evidently depends on whether $5\sigma_{0R}^2 - 1$ is positive or negative. For the TM_1-mode $5\sigma_{0R}^2 - 1$ is negative, and therefore $\Delta\gamma_R/j$ is positive, for the TM_2- and TM_3-modes, however, $5\sigma_{0R}^2 - 1$ is positive and $\Delta\gamma_R/j$ negative. This also is in accordance with our previous observations and explains the anomaly pointed out above. The equation (78) does not hold for $n = 0$. In this case $\sigma_{0R} = 0$ and the approximation is no longer valid.

P r o p a g a t i o n p e r p e n d i c u l a r t o t h e g y r o - a x i s. We shall now consider in some detail the modes propagated in the direction $+y$ (see fig. 5). Again we start from the general equations (14) and (17). In this case the field components are independent of z, i.e. $\partial/\partial z \equiv -\gamma = 0$, and on account of this some of the constants in (14) and (17) disappear. Comparison with the definitions (11) and (15) shows that $p = q = b = d = 0$. The differential equations for E_z and H_z then are

$$[\nabla_t^2 + \omega^2\varepsilon_3\,(\mu_1^2 - \mu_2^2)/\mu_1]\,E_z = 0, \quad [\nabla_t^2 + \omega^2\mu_3\,(\varepsilon_1^2 - \varepsilon_2^2)/\varepsilon_1]\,H_z = 0, \tag{2.75}$$

and the expressions for the transverse fields become

$$\mathbf{E}_t = r\,\nabla_t H_z - s\,\mathbf{k} \times \nabla_t H_z, \quad \mathbf{H}_t = t\,\nabla_t E_z - u\,\mathbf{k} \times \nabla_t E_z. \tag{2.76}$$

The modes in this case are either TM, with the components $H_z\mathbf{k}$ and $\mathbf{E}_t$, or TE, with the components $E_z\,\mathbf{k}$ and $\mathbf{H}_t$. We shall consider the two types separately.

a) TM-m o d e s. Suppose the y-dependence of the components is described by the factor exp $(-\gamma' y)$. Then $\partial/\partial y \equiv -\gamma'$, and H_z must satisfy the equation

$$(\mathrm{d}^2/\mathrm{d}x^2 + \sigma'^2)\,H_z = 0, \quad \sigma'^2 = \gamma'^2 + \omega^2\mu_3(\varepsilon_1^2 - \varepsilon_2^2)/\varepsilon_1. \tag{2.77}$$

Moreover it is subject to the boundary condition

$$(\partial H_z/\partial x)_{x=\pm x_0} = 0. \tag{2.78}$$

Then the particular solutions of (77) are easily found to be

$$H_{zn} = [\exp(j\sigma_n' x) + (-)^n \exp(-j\sigma_n' x)] \exp(-\gamma_n' y), \tag{2.79}$$

where $\sigma_n' = n\pi/2x_0$. The other components follow from (76):

$$E_{xn} = r\,\partial H_{zn}/\partial x - s\gamma_n' H_{zn}, \quad E_{yn} = -r\,\gamma_n' H_{zn} - s\,\partial H_{zn}/\partial x. \tag{2.80}$$

b) TE-m o d e s. Suppose $\partial/\partial y \equiv -\gamma''$; then E_z must be a solution of

$$(\mathrm{d}^2/\mathrm{d}x^2 + \sigma''^2)\,E_z = 0, \quad \sigma''^2 = \gamma''^2 + \omega^2\varepsilon_3(\mu_1^2 - \mu_2^2)/\mu_1. \tag{2.81}$$

The boundary condition for E_z is

$$(E_z)_{x=\pm x_0} = 0. \tag{2.82}$$

From (81) and (82) we find in the familiar way

$$E_{zn} = [\exp(j\sigma_n'' x) - (-)^n \exp(-j\sigma_n'' x)] \exp(-\gamma_n'' y), \tag{2.83}$$

where $\sigma_n'' = n\pi/2x_0$. On account of (76) we have

$$\left.\begin{aligned} H_{xn} &= t\,\partial E_{zn}/\partial x - u\gamma_n'' E_{zn} = \\ &= \{j\sigma_n'' t\,[\exp(j\sigma_n'' x) + (-)^n \exp(-j\sigma_n'' x)] - \\ &\quad - u\gamma_n''[\exp(j\sigma_n'' x) - (-)^n \exp(-j\sigma_n'' x)]\} \exp(-\gamma_n'' y) \\ H_{yn} &= -t\gamma_n'' E_{zn} - u\,\partial E_{zn}/\partial x = \\ &= \{-t\gamma_n''[\exp(j\sigma_n'' x) - (-)^n \exp(-j\sigma_n'' x)] - \\ &\quad - j\sigma_n'' u\,[\exp(j\sigma_n'' x) + (-)^n \exp(-j\sigma_n'' x)]\} \exp(-\gamma_n'' y). \end{aligned}\right\} \tag{2.84}$$

Moreover

$$B_{xn} = (\gamma_n''/j\omega)\,E_{zn}, \quad B_{yn} = (1/j\omega)\,\partial E_{zn}/\partial x. \tag{2.85}$$

We have written out these components in somewhat more detail than for the TM-modes as they describe also a series of modes in wave guides of rectangular cross-section. Let us remember that the field components are independent of z and that we have only E_z, H_x and H_y (see fig. 8*a*). Evidently we can place perfectly conducting planes perpendicular to the z-axis without interfering with our solutions; the boundary conditions on these planes $\mathbf{E}_t = B_z\mathbf{k} = 0$ are satisfied. Placing two such planes at $z = \pm z_0$ we form in effect a wave guide of rectangular cross-section as shown in fig. 8*b*. The solutions (83)–(85) then represent TE_{0n}-waves in rectangular wave guides containing gyro-media with the gyro-axis in the z-direction.

We may well add here some remarks concerning a boundary value problem connected with these rectangular wave guides. Suppose the wave guide contains air for $y < 0$ and the gyro-medium for $y > 0$. At the boundary $y = 0$ the components E_z, H_x and B_y must be continuous. Let us now compare the components of TE_{01}-modes in air and in the medium. From the definitions (11), where now $\gamma = 0$, we obtain

$$u = -\mu_1/j\omega(\mu_1^2 - \mu_2^2), \qquad t = \mu_2/\omega(\mu_1^2 - \mu_2^2). \tag{2.86}$$

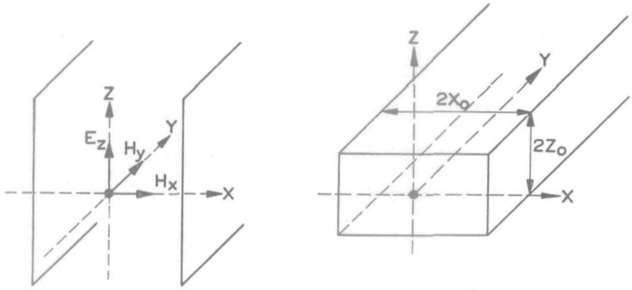

Fig. 8. *a*. Field components of TE_1-mode between two parallel planes. *b*. Rectangular wave guide.

Denoting by subscripts m and a quantities referring to the medium, c.q. to air we find from (83)–(85)

$$\left.\begin{aligned}
&E_{za} = A_a \cos(\pi x/2x_0), \qquad E_{zm} = A_m \cos(\pi x/2x_0),\\
&H_{xa} = (\gamma_a/j\omega)\, A_a \cos(\pi x/2x_0),\\
&H_{xm} = (\gamma_m/j\omega)\,[\mu_1/(\mu_1^2 - \mu_2^2)]\, A_m \cos(\pi x/2x_0) -\\
&\quad - \omega^{-1}(\pi/2x_0)\,[\mu_2/(\mu_1^2 - \mu_2^2)]\, A_m \sin(\pi x/2x_0),\\
&B_{ya} = -(\pi/j\omega 2x_0)\, A_a \sin(\pi x/2x_0),\\
&B_{ym} = j\omega^{-1}(\pi/2x_0)\, A_m \sin(\pi x/2x_0).
\end{aligned}\right\} \tag{2.87}$$

When we try to satisfy the boundary conditions at $y = 0$ with these two wave types, the components E_z and B_y do not cause any complications as they have the same x-dependence in both types. The H_{xm} component, however, contains in addition to the cosine term, which is also present in H_{xa}, a sine term, and on account of this sine term it is impossible to satisfy the boundary conditions at $y = 0$ with

TE_{01}-modes only. In other words: at the discontinuity $y = 0$ a TE_{01}-wave, incident from $z = -\infty$, gives rise not only to transmitted and reflected TE_{01}-waves, but to other modes as well. In principle the boundary value problem can be solved by assuming infinite series of TE_{0n}-waves in both reflection and transmission. One is led to an infinite system of linear equations which is difficult to handle.

§ 7. *Wave guides of circular cross-section.* In dealing with this configuration we naturally use cylindrical coordinates ϱ, ϑ, z, as shown in fig. 9. Let the radius of the cylinder be ϱ_0. Again we shall simply apply the results of the general theory, which was set up in

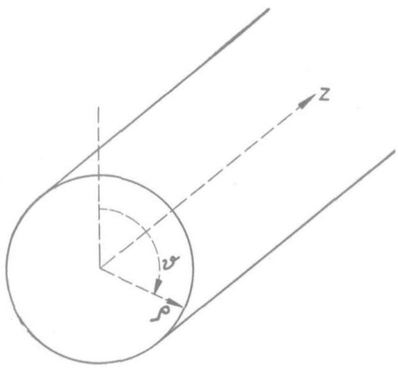

Fig. 9. Cylindrical coordinates.

generalized orthogonal cylindrical coordinates. We remark that in this case $h_1 dv_1 = d\varrho$, $h_2 dv_2 = \varrho d\vartheta$, i.e.

$$h_1 = 1, \; h_2 = \varrho. \tag{2.88}$$

We shall distinguish between completely filled wave guides and wave guides containing a coaxial anisotropic cylinder, radius $\varrho_1 < \varrho_0$, embedded in air. The characteristic equations for γ, the roots of which represent the propagation constants of the modes, were derived by Suhl and Walker [29]) for a completely filled wave guide containing a medium which is both gyromagnetic and gyroelectric, and by Kales [13]) for completely and partially filled wave guides containing gyromagnetic media. Here we shall derive these results briefly from our general theory, and then we shall investigate more carefully the case of a partially filled wave guide containing very thin gyromagnetic cylinders ($\varrho_1 \ll \varrho_0$). These considerations will suggest an experimental method for determining the elements of the μ-tensor separately.

Completely filled circular wave guides. The differential equations for $\varphi_{1,2}$ now have the form

$$\left(\frac{\partial^2}{\partial \varrho^2} + \frac{1}{\varrho}\frac{\partial}{\partial \varrho} + \frac{1}{\varrho^2}\frac{\partial^2}{\partial \vartheta^2} + \sigma_{1,2}^2\right)\varphi_{1,2} = 0. \tag{2.89}$$

This equation has the solutions

$$\varphi_{1,2} = A_{1,2}\, J_n(\sigma_{1,2}\varrho) \exp jn\vartheta, \qquad n = 0, \pm 1, \pm 2, \ldots \tag{2.90}$$

We have written here exp $jn\vartheta$, rather than cos $n\vartheta$ or sin $n\vartheta$, for a reason which will soon be evident. The Neumann function can be omitted on account of its singularity at the origin. We shall try to solve the boundary value problem with φ-functions containing only one n: then e.g.

$$E_z = A_1 J_n(\sigma_1\varrho) \exp jn\vartheta + A_2 J_n(\sigma_2\varrho) \exp jn\vartheta. \tag{2.91}$$

The other field components follow at once from (32) and (17), and the boundary conditions for $\varrho = \varrho_0$ can be found from (38). Noticing that in this case $\partial/\partial\nu \equiv \partial/\partial\varrho$; $\partial/\partial\tau \equiv \varrho^{-1}\partial/\partial\vartheta$ we obtain

$$\left.\begin{aligned} &[A_1 J_n(\sigma_1\varrho_0) + A_2 J_n(\sigma_2\varrho_0)] \exp jn\vartheta = 0, \\ &\{A_1\, [(jnr/\varrho_0)\, \sigma_2^2 J_n(\sigma_1\varrho_0) - \sigma_1(s\sigma_2^2 + j\omega\mu_3)\, J_n'(\sigma_1\varrho_0)] + \\ &\quad + A_2[(jnr/\varrho_0)\sigma_1^2 J_n(\sigma_2\varrho_0) - \sigma_2(s\sigma_1^2 + j\omega\mu_3) J_n'(\sigma_2\varrho_0)]\} \exp jn\vartheta = 0. \end{aligned}\right\} \tag{2.92}$$

Here the primes mean differentiations with respect to the arguments of the Bessel functions. From (92) we derive in the now familiar way the characteristic equation

$$\begin{aligned} &(jnr/\varrho_0)\,(\sigma_1^2 - \sigma_2^2) + \\ &+ \sigma_1(s\sigma_2^2 + j\omega\mu_3) J_n'(\sigma_1\varrho_0)/J_n(\sigma_1\varrho_0) - \sigma_2(s\sigma_1^2 + j\omega\mu_3) J_n'(\sigma_2\varrho_0)/J_n(\sigma_2\varrho_0) = 0. \end{aligned} \tag{2.93}$$

This equation can also be solved graphically to give the propagation constants of the modes for each specific value of n. We notice immediately that the equation is not even in n; this means that the propagation constants for the right and left circularly polarized modes are different. We also notice that the derivation of (93) would have been impossible if we had not been able to divide (92) by exp $jn\vartheta$. Starting from φ-functions containing cos $n\vartheta$ or sin $n\vartheta$

only we would have obtained different ϑ-factors in the second equation of (92), and this would have resulted in $A_1 = A_2 = 0$. As in the case of guided waves between two parallel planes of infinite extent, it may be shown that the modes in circular wave guides containing gyro-media may be divided into two groups, viz. quasi-TM- and quasi-TE-modes, which become TM and TE when the anisotropy is gradually removed.

All this furnishes us with the following picture of the Faraday rotation of guided waves in a circular cylinder of a gyro-medium which fills the wave guide for $z > 0$, whereas for $z < 0$ there is air. Suppose a "linearly" polarized TE_{11}-wave is incident from $z = -\infty$. This wave may be decomposed mathematically into a right and left circularly polarized TE_{11}-wave of equal amplitudes. The transmitted wave in the anisotropic medium will mainly consist of quasi-TE_{11}-circularly polarized waves. As long as the anisotropy is small, the transmission coefficients for the two circularly polarized component waves will be nearly the same, and the slight difference in propagation constants in the anisotropic medium will result in a small Faraday rotation of the nearly linearly polarized transmitted wave. In case of large anisotropies, however, the transmission coefficients will not be the same for the two circularly polarized waves, and the reflected and transmitted waves will no longer be linearly polarized. Moreover the transverse fields in the TE_{11}-mode ($z < 0$) and the quasi-TE_{11}-mode ($z > 0$) cannot be made to match at $z = 0$ (cf. § 6), so that other modes will be excited at the transition. In view of all this one has to be very careful in the interpretation of experimental data on magnetic Faraday rotation in completely filled wave guides, and we are not aware at present of any measurements which have been analyzed in a physically satisfactory way.

Partially filled circular wave guides. We now turn to the case of a wave guide of circular cross-section which contains a coaxial cylinder of radius $\varrho_1 < \varrho_0$ of a gyro-medium. We suppose that there is air for $\varrho_1 < \varrho < \varrho_0$ (see fig. 10). We shall denote the field components in the anisotropic medium by a superscript m, in air by a superscript a. The φ-functions in the gyro-medium again satisfy (89). From (32) and (90) we find E_z^m and H_z^m:

$$\left.\begin{aligned} E_z^m &= [A_1 J_n(\sigma_1\varrho) + A_2 J_n(\sigma_2\varrho)] \exp jn\vartheta, \\ H_z^m &= b^{-1} [(\sigma_1^2 - a) A_1 J_n(\sigma_1\varrho) + (\sigma_2^2 - a) A_2 J_n(\sigma_2\varrho)] \exp jn\vartheta. \end{aligned}\right\} \quad (2.94)$$

In air the longitudinal components must satisfy the wave equation

$$\left(\frac{\partial^2}{\partial \varrho^2} + \frac{1}{\varrho}\frac{\partial}{\partial \varrho} + \frac{1}{\varrho^2}\frac{\partial^2}{\partial \vartheta^2} + \sigma^2\right) E_z^a,\ H_z^a = 0, \tag{2.95}$$

where

$$\sigma^2 = \omega^2 \varepsilon_0 \mu_0 + \gamma^2. \tag{2.96}$$

In the general solutions of (95) Neumann functions appear, as the air region does not include the axis $\varrho = 0$. Thus we find

$$\left.\begin{aligned} E_z^a &= [A_3' J_n(\sigma\varrho) + A_3'' N_n(\sigma\varrho)] \exp jn\vartheta \cancel{= 0}, \\ H_z^a &= [A_4' J_n(\sigma\varrho) + A_4'' N_n(\sigma\varrho)] \exp jn\vartheta \cancel{= 0}. \end{aligned}\right\} \tag{2.97}$$

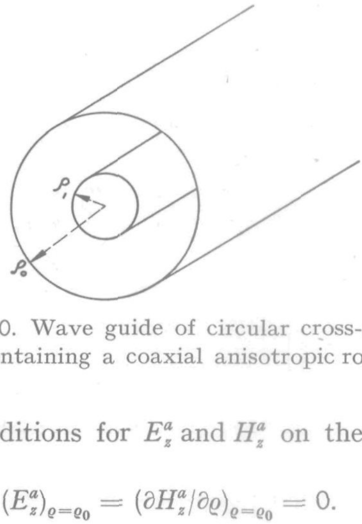

Fig. 10. Wave guide of circular cross-section containing a coaxial anisotropic rod.

The boundary conditions for E_z^a and H_z^a on the wave guide wall require that

$$(E_z^a)_{\varrho=\varrho_0} = (\partial H_z^a/\partial \varrho)_{\varrho=\varrho_0} = 0. \tag{2.98}$$

?

Substituting (97) in (98) we find at once

$$A_3''/A_3' = -\,J_n(\sigma\varrho_0)/N_n(\sigma\varrho_0), \quad A_4''/A_4' = -\,J_n'(\sigma\varrho_0)/N_n'(\sigma\varrho_0). \tag{2.99}$$

We then rewrite (97) as

$$E_z^a = A_3 F(\varrho) \exp jn\vartheta, \qquad H_z^a = A_4 G(\varrho) \exp jn\vartheta, \tag{2.100}$$

where

$$\left.\begin{aligned} F(\varrho) &= N_n(\sigma\varrho_0)\, J_n(\sigma\varrho) - J_n(\sigma\varrho_0)\, N_n(\sigma\varrho), \\ G(\varrho) &= N_n'(\sigma\varrho_0)\, J_n(\sigma\varrho) - J_n'(\sigma\varrho_0)\, N_n(\sigma\varrho). \end{aligned}\right\} \tag{2.101}$$

In addition to the boundary conditions at the wave guide wall, which we have satisfied by (99), we now have the conditions that for $\varrho = \varrho_1$ the components E_z, H_z, E_ϑ and H_ϑ are continuous. These four conditions give four linear relations in A_1, A_2, A_3 and A_4, and in the familiar way we can derive a characteristic equation for γ. Again it is essential, as one will notice, that the ϑ-dependence of the components is assumed to be exp $jn\vartheta$. In order to find E_ϑ and H_ϑ we use (34), (35) and the definitions (11) and (15):

$$\left.\begin{aligned} E_\vartheta^a &= \left[-\frac{jn}{\varrho}\frac{\gamma}{\sigma^2}A_3F(\varrho) + \frac{j\omega\mu_0}{\sigma^2}A_4G'(\varrho)\right]\exp jn\vartheta, \\ H_\vartheta^a &= \left[-\frac{jn}{\varrho}\frac{\gamma}{\sigma^2}A_4G(\varrho) - \frac{j\omega\varepsilon_0}{\sigma^2}A_3F'(\varrho)\right]\exp jn\vartheta, \end{aligned}\right\} \tag{2.102}$$

$$\left.\begin{aligned} E_\vartheta^m = b^{-1}\Big\{\frac{jn}{\varrho}\Big[&\Big(-\omega\mu_3\frac{\varepsilon_2}{\varepsilon_1} - r\sigma_2^2\Big)A_1J_n(\sigma_1\varrho) + \\ &+ \Big(-\omega\mu_3\frac{\varepsilon_2}{\varepsilon_1} - r\sigma_1^2\Big)A_2J_n(\sigma_2\varrho)\Big] + (j\omega\mu_3 + s\sigma_2^2)\,\sigma_1A_1J_n'(\sigma_1\varrho) + \\ &+ (j\omega\mu_3 + s\sigma_1^2)\,\sigma_2A_2J_n'(\sigma_2\varrho)\Big\}\exp jn\vartheta, \\ H_\vartheta^m = b^{-1}\Big\{\frac{jn}{\varrho}\Big[&\Big(-\gamma\frac{\mu_3}{\mu_1} - p\sigma_2^2\Big)A_1J_n(\sigma_1\varrho) + \\ &+ \Big(-\gamma\frac{\mu_3}{\mu_1} - p\sigma_2^2\Big)A_2J_n(\sigma_2\varrho)\Big] + q\sigma_2^2\sigma_1A_1J_n'(\sigma_1\varrho) + \\ &+ q\sigma_1^2\sigma_2A_2J_n'(\sigma_2\varrho)\Big\}\exp jn\vartheta. \end{aligned}\right\} \tag{2.103}$$

Now we first write down the boundary conditions for E_z and H_z; from (94) and (100) we obtain

$$\left.\begin{aligned} A_3F(\varrho_1) &= A_1J_n(\sigma_1\varrho_1) + A_2J_n(\sigma_2\varrho_1), \\ A_4G(\varrho_1) &= b^{-1}[(\sigma_1^2 - a)A_1J_n(\sigma_1\varrho_1) + (\sigma_2^2 - a)A_2J_n(\sigma_2\varrho_1)] = \\ &= b^{-1}[(c - \sigma_2^2)A_1J_n(\sigma_1\varrho_1) + (c - \sigma_2^2)A_2J_n(\sigma_2\varrho_1)]. \end{aligned}\right\} \tag{2.104}$$

Next we consider the boundary conditions for E_ϑ and H_ϑ. Substituting A_3 and A_4 from (104) we find two relations of the form

$$O_1A_1 + O_2A_2 = 0,\ P_1A_1 + P_2A_2 = 0, \tag{2.105}$$

where

$$O_{1,2} = \Big[-\frac{jn}{\varrho_1}\frac{\gamma}{\sigma^2} + \frac{j\omega\mu_0}{\sigma^2}\frac{c-\sigma_{2,1}^2}{b}\frac{G'(\varrho_1)}{G(\varrho_1)} + \\ + \frac{jn}{b\varrho_1}\Big(\omega\mu_3\frac{\varepsilon_2}{\varepsilon_1} + r\sigma_{2,1}^2\Big)\Big] J_n(\sigma_{1,2}\,\varrho_1) + \\ - b^{-1}(j\omega\mu_3 + s\sigma_{2,1}^2)\,\sigma_{1,2} J_n'(\sigma_{1,2}\,\varrho_1), \tag{2.106a}$$

$$P_{1,2} = \Big[-\frac{jn}{\varrho_1}\frac{\gamma}{\sigma^2}\frac{c-\sigma_{2,1}^2}{b} - \frac{j\omega\varepsilon_0}{\sigma^2}\frac{F'(\varrho_1)}{F(\varrho_1)} + \\ + \frac{jn}{b\varrho_1}\Big(\gamma\frac{\mu_3}{\mu_1} + p\sigma_{2,1}^2\Big)\Big] J_n(\sigma_{1,2}\,\varrho_1) - b^{-1} q\sigma_{2,1}^2\,\sigma_{1,2} J_n'(\sigma_{1,2}\varrho_1). \tag{2.106b}$$

The first indices refer to O_1 and P_1, the second to O_2 and P_2. The characteristic equation for γ then becomes

$$O_1P_2 - O_2P_1 = 0. \tag{2.107}$$

This equation reduces to (93) when $\varrho_1 \to \varrho_0$; it is easily verified that $F(\varrho_0) = G'(\varrho_0) = 0$, whereas $F'(\varrho_0) = -\sigma G(\varrho_0)$ is finite. About (107) we can make the same remarks which have been made above concerning (93). The characteristic equations for $+n$ and $-n$ are not identical, and this again gives us a description of the Faraday rotation of guided waves.

Approximation for thin cylinders ($\varrho_1 \ll \varrho_0$). We finally work out a first order approximation for the solution of (107) for the case of a thin coaxial cylinder for a medium which is gyromagnetic only. This is of practical importance as regards our experiments on Faraday rotation (cf. Chapter IV and V). We restrict our treatment to quasi-TE_{11}-modes with ϑ-dependences exp $(\pm j\vartheta)$. In the following expressions upper signs will correspond to exp $(+j\vartheta)$, lower signs to exp $(-j\vartheta)$. When $\varrho_1 \ll \varrho_0$, the propagation constants of the circularly polarized waves will approach γ_0, the propagation constant of a TE_{11}-mode in an air-filled circular wave guide of radius ϱ_0. This γ_0 satisfies the equation

$$\gamma_0^2 + \omega^2\varepsilon_0\mu_0 = \sigma_0^2, \tag{2.108}$$

where σ_0 is the first root of $J_1'(\sigma\varrho_0) = 0$. The constant σ of (95) will approach σ_0; so, if we write $\gamma = \gamma_0 + \Delta\gamma$, $\sigma = \sigma_0 + \Delta\sigma$, we obtain from (96) and (108)

$$\sigma_0\,\Delta\sigma \simeq \gamma_0\,\Delta\gamma. \tag{2.109}$$

We now consider (107) for small ϱ_1; from the definitions of Bessel and Neumann functions *), as given by Jahnke and Emde[12]), we obtain for $x \ll 1$

$$\left.\begin{aligned} J_1(x) &\simeq (x/2)\,[1-\tfrac{1}{2}(x/2)^2], \quad xJ_1'(x) \simeq J_1(x)\,[1-(x/2)^2], \\ \pi N_1(x) &\simeq -(2/x)\,[1-2(x/2)^2 \ln(\varkappa x/2) + (x/2)^2], \\ -x\pi N_1'(x) &\simeq -(2/x)\,[1+2(x/2)^2 \ln(\varkappa x/2) + (x/2)^2]. \end{aligned}\right\} \quad (2.110)$$

Moreover we have $J_1(x) = -J_{-1}(x)$, $N_1(x) = -N_{-1}(x)$. Using these expressions and the definitions (101) we derive

$$\frac{F'(\varrho_1)}{F(\varrho_1)} \equiv \frac{1}{\varrho_1}\frac{\Phi_F}{\Psi_F} =$$

$$= \frac{1}{\varrho_1}\frac{\pi N_1(\sigma\varrho_0)(\sigma\varrho_1/2)^2 - J_1(\sigma\varrho_0)[1+2(\sigma\varrho_1/2)^2\ln(\varkappa\sigma\varrho_1/2)+(\sigma\varrho_1/2)^2]}{\pi N_1(\sigma\varrho_0)(\sigma\varrho_1/2)^2 + J_1(\sigma\varrho_0)[1-2(\sigma\varrho_1/2)^2\ln(\varkappa\sigma\varrho_1/2)+(\sigma\varrho_1/2)^2]}, \quad (2.111a)$$

$$\frac{G'(\varrho_1)}{G(\varrho_1)} \equiv \frac{1}{\varrho_1}\frac{\Phi_G}{\Psi_G} =$$

$$= \frac{1}{\varrho_1}\frac{\pi N_1'(\sigma\varrho_0)(\sigma\varrho_1/2)^2 - J_1'(\sigma\varrho_0)[1+2(\sigma\varrho_1/2)^2\ln(\varkappa\sigma\varrho_1/2)+(\sigma\varrho_1/2)^2]}{\pi N_1'(\sigma\varrho_0)(\sigma\varrho_1/2)^2 + J_1'(\sigma\varrho_0)[1-2(\sigma\varrho_1/2)^2\ln(\varkappa\sigma\varrho_1/2)+(\sigma\varrho_1/2)^2]}. \quad (2.111b)$$

From (106), (110) and (111) we find for the TE_{11}-modes

$$O_{1,2} = \pm \frac{j}{b\varrho_1} J_1(\sigma_{1,2}\varrho_1) \Big\{ \mp \frac{b\gamma}{\sigma^2} + \frac{\omega\mu_0}{\sigma^2}(c-\sigma_{2,1}^2)\frac{\Phi_G}{\Psi_G} \pm$$

$$\pm r\sigma_{2,1}^2 - (\omega\mu_3 - js\sigma_{2,1}^2)\,[1-(\sigma_{1,2}\varrho_1/2)^2]\Big\}, \quad (2.112a)$$

$$P_{1,2} = \pm \frac{j}{b\varrho_1} J_1(\sigma_{1,2}\varrho_1) \Big\{ \mp \frac{\gamma}{\sigma^2}(c-\sigma_{2,1}^2) - \frac{\omega\varepsilon_0 b}{\sigma^2}\frac{\Phi_F}{\Psi_F} \pm$$

$$\pm \gamma\frac{\mu_3}{\mu_1} \pm p\sigma_{2,1}^2 + jq\sigma_{2,1}^2\,[1-(\sigma_{1,2}\varrho_1/2)^2]\Big\}. \quad (2.112b)$$

Substituting (112) in (107) it is a matter of algebra to show that we can separate from (107) the factor $b^{-1}(\sigma\varrho_1)^{-2}\,(\sigma_1^2-\sigma_2^2)J_1(\sigma_1\varrho_1)J_1(\sigma_2\varrho_1)$, and we are then left with an equation of the form

$$\Phi_F\Phi_G W_1 + \Psi_F\Phi_G W_2 + \Phi_F\Psi_G W_3 + \Psi_F\Psi_G W_4 = 0, \quad (2.113)$$

*) In order to avoid confusion with the propagation constant γ, Euler's constant here is denoted as $\varkappa$.

where

$$W_1 = \frac{\omega^2 \varepsilon_0 \mu_0}{\sigma^2},$$

$$\left.\begin{aligned} W_2 &= -\omega^2 \varepsilon \mu_0 \left[\frac{1}{\gamma^2 + \omega^2 \varepsilon(\mu_1 \pm \mu_2)} - \left(\frac{\varrho_1}{2}\right)^2\right], \\ W_3 &= -\omega^2 \varepsilon_0 \left[\frac{\mu_1 \pm \mu_2}{\gamma^2 + \omega^2 \varepsilon(\mu_1 \pm \mu_2)} - \mu_3 \left(\frac{\varrho_1}{2}\right)^2\right], \\ W_4 &= \frac{\sigma^2 - 2\gamma^2}{\gamma^2 + \omega^2 \varepsilon(\mu_1 \pm \mu_2)} + \frac{\gamma^2}{\sigma^2} - (\tfrac{1}{2}\sigma\varrho_1)^2 \frac{\omega^2 \varepsilon(\mu_1 \pm \mu_2 + \mu_3)}{\gamma^2 + \omega^2 \varepsilon(\mu_1 \pm \mu_2)}. \end{aligned}\right\} \tag{2.114}$$

From (111) and (113) we finally obtain the characteristic equation

$$\begin{aligned} &J_1'(\sigma\varrho_0)\, J_1(\sigma\varrho_0)\, \{[1 + 2(\sigma\varrho_1/2)^2]\, (W_1 - W_2 - W_3 + W_4) + \\ &\qquad + 4(\sigma\varrho_1/2)^2 \ln(\varkappa\sigma\varrho_1/2)\, (W_1 - W_4)\} + \\ &+ \pi J_1'(\sigma\varrho_0)\, N_1(\sigma\varrho_0)\, (\sigma\varrho_1/2)^2\, (-W_1 - W_2 + W_3 + W_4) + \\ &+ \pi J_1(\sigma\varrho_0)\, N_1'(\sigma\varrho_0)\, (\sigma\varrho_1/2)^2\, (-W_1 + W_2 - W_3 + W_4) = 0. \end{aligned} \tag{2.115}$$

0^{th} order approximation. Neglecting in (115) all but the terms of degree zero in ϱ_1 we have

$$J_1'(\sigma\varrho_0) = 0, \tag{2.116a}$$

or

$$J_1(\sigma\varrho_0) = 0. \tag{2.116b}$$

The roots of (116*a*) correspond to TE-modes, the roots of (116*b*) to TM-modes.

1st order approximation. As we are interested in the quasi TE_{11}-modes, we can put $\sigma = \sigma_0 + \Delta\sigma$, where σ_0 is the first root of $J_1'(\sigma\varrho_0) = 0$. Then $J_1'(\sigma\varrho_0) \simeq \Delta\sigma\varrho_0\, J_1''(\sigma_0\varrho_0)$. Substituting this into (115) we get

$$\begin{aligned} \Delta\sigma &\simeq \frac{\pi N_1'(\sigma_0\varrho_0)}{\varrho_0 J_1''(\sigma_0\varrho_0)} \left(\frac{\sigma_0\,\varrho_1}{2}\right)^2 \frac{W_1 - W_2 + W_3 - W_4}{W_1 - W_2 - W_3 + W_4} \\ &\simeq \frac{\pi N_1'(\sigma_0\,\varrho_0)}{4\varrho_0 J_1''(\sigma_0\,\varrho_0)} \cdot \\ &\cdot \varrho_1^2 \frac{\gamma_0^2(\varepsilon + \varepsilon_0)\,[\mu_0 - (\mu_1 \pm \mu_2)] + \omega^2 \varepsilon_0\,\mu_0\,(\varepsilon - \varepsilon_0)\,(\mu_0 + \mu_1 \pm \mu_2)}{(\varepsilon + \varepsilon_0)\,(\mu_0 + \mu_1 \pm \mu_2)}. \end{aligned} \tag{2.117}$$

On account of (109) we can then write

$$\varrho_1^{-2}\Delta\gamma_\pm = \frac{\sigma_0}{\gamma_0}\frac{\pi N_1'(\sigma_0\varrho_0)}{4\varrho_0 J_1''(\sigma_0\varrho_0)}\left[-\gamma_0^2\frac{\mu_1\pm\mu_2-\mu_0}{\mu_1\pm\mu_2+\mu_0}+\omega^2\varepsilon_0\mu_0\frac{\varepsilon-\varepsilon_0}{\varepsilon+\varepsilon_0}\right]. \quad (2.118)$$

Thus we see that for small diameters $\Delta\gamma$ is proportional to ϱ_1^2. The left hand side can be determined from experiments and will be used to find experimental values of μ_1 and μ_2.

CHAPTER III. EXPERIMENTAL DETAILS

In the preceding chapter we have made a theoretical investigation of wave propagation in wave guides containing anisotropic media. We shall now give an account of some experiments on magnetic Faraday rotation in ferrites. In § 3 we have briefly described the work of previous investigators who measured the Faraday rotation of guided waves as a function of a constant axial magnetic field H_c in a direct way. In § 7, however, we have pointed out that difficulties arise in the interpretation of such measurements. Moreover, there are some experimental drawbacks. First of all it is hard to avoid reflections in the different transition regions in a Faraday rotator; secondly small rotations cannot be measured accurately, and finally small attenuation constants cannot be determined at all. In this chapter we shall first describe a new technique for measuring Faraday rotations; next we shall discuss the experimental arrangement used and the materials investigated.

§ 8. *A cavity technique for measuring Faraday rotations* [32]). When studying the case of a wave guide of circular cross-section containing a coaxial cylinder of a gyro-magnetic medium, we have seen that there are solutions with ϑ-factors exp $(\pm\, jn\vartheta)$. The transverse electric fields, for example, have the form

$$\mathbf{E}_{t+} = \hat{\mathbf{E}}_{t+} \exp j(n\vartheta - \beta_+ z), \quad \mathbf{E}_{t-} = \hat{\mathbf{E}}_{t-} \exp j(-n\vartheta - \beta_- z). \quad (3.1)$$

On account of the anisotropy $\beta_+ \neq \beta_-$. Les us now take $n=1$ and $\hat{\mathbf{E}}_{t+} = \hat{\mathbf{E}}_{t-}$, and let us consider the superposition of these waves. The transverse electric field then is

$$\mathbf{E}_t = \hat{\mathbf{E}}_t \{\exp(j\vartheta - j\beta_+ z) + \exp(-j\vartheta - j\beta_- z)\}. \quad (3.2)$$

For $z=0$

$$\mathbf{E}_t(0) = 2\hat{\mathbf{E}}_t \cos\vartheta. \quad (3.3)$$

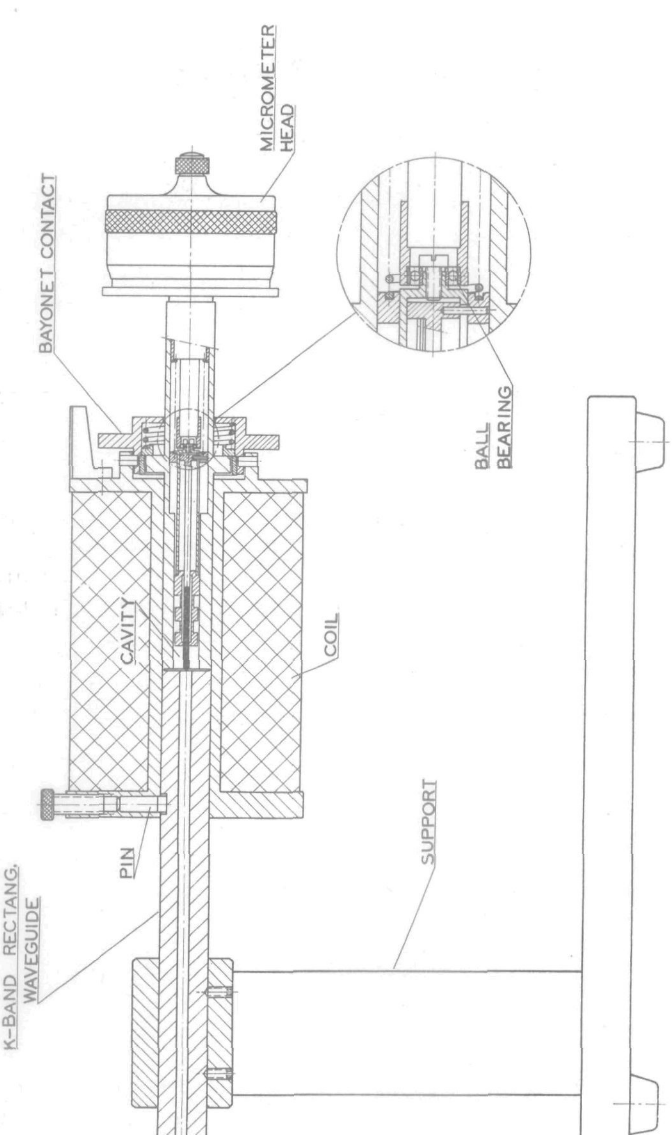

Fig. 11. Detailed drawing of K-band cavity.

This is a maximum for $\vartheta = 0$ or π, and we call $\vartheta = 0$ the direction of polarization. For $z = 1$

$$\mathbf{E}_t(1) = 2\hat{\mathbf{E}}_t \exp\{-\tfrac{1}{2}j(\beta_- + \beta_+)\} \cos\{\vartheta + \tfrac{1}{2}(\beta_- - \beta_+)\}. \quad (3.4)$$

Here the direction of polarization is given by $\vartheta = -\frac{1}{2}(\beta_- - \beta_+)$, and the Faraday rotation per unit length Θ is

$$\Theta = \tfrac{1}{2}(\beta_+ - \beta_-). \tag{3.5}$$

By measuring Faraday rotations directly we actually determine the difference of β_+ and β_-. It would be more informative, however, to find β_+ and β_- separately. This point, together with the disadvantages mentioned above, which are inherent in the rotator technique, has led us to develop another technique, limited, it is true, in its applicability, but more satisfactory from a physical point of view. A ferrite rod is mounted coaxially in a cylindrical cavity which can be tuned by means of a movable plunger. The plunger has a hole in it that fits around the ferrite. Fig. 11 shows a drawing of the K-band cavity used. When the ferrite is not magnetized, resonances will occur at distances of $\lambda_g/2$, where $\lambda_g = 2\pi/\beta$ and $\beta = \beta_+ = \beta_-$. An axial constant magnetic field causes splitting of these resonances since the propagation constants β_+ and β_- are then no longer equal. Attenuation constants can be found from Q-measurements.

The excitation of the cavity is achieved by means of two symmetrical coupling holes which connect the cavity with the feeding

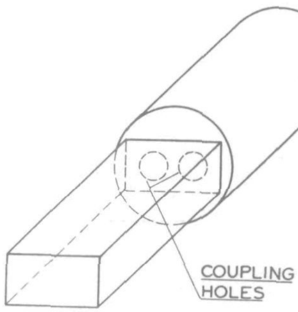

Fig. 12. Coupling between rectangular wave guide and cavity.

rectangular wave guide (see fig. 12). In this type of coupling the right and left circularly polarized waves are excited equally. In case of small resonance splitting and high losses, i.e. low Q's, this can be prohibitive since the two resonances are then no longer resolved. This disadvantage is not essential, however, since it is possible to excite each one of the circularly polarized waves by itself. The hole in the plunger sets an upper limit to the rod diameters that can be employed in the technique described here: it must be a wave guide below cutoff in order to prevent unwanted loading of the cavity. This restriction clearly is a fundamental one.

Summarizing we can say that the cavity technique has the following features:

a) It allows to measure β_+ and β_-, and therefore Θ, very accurately.

b) Small attenuation constants can be determined.

c) The matching problem of the rotator technique is eliminated.

d) It is useful for small rod diameters only.

e) Special provisions have to be made in case of high attenuation and small resonance splitting.

§ 9. *Experimental arrangement.* The apparatus used consists of a wave guide system and the electronic equipment required for power supply and detection. In fig. 13 a block diagram is shown. We shall

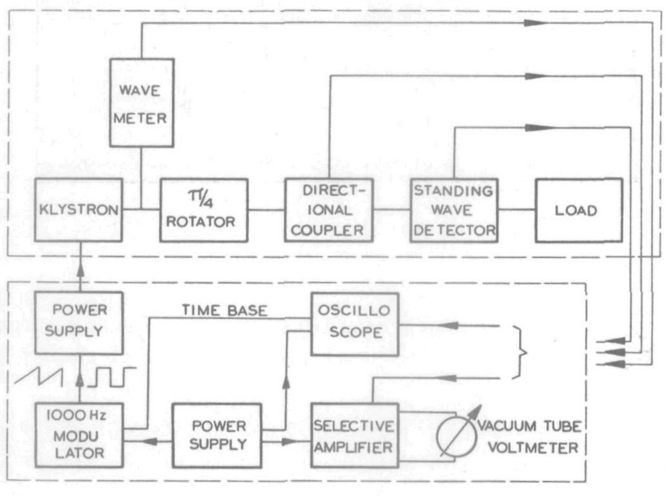

Fig. 13. Block diagram of experimental arrangement.

briefly discuss the various elements. As an oscillator we used a 2 K 33 Raytheon reflex klystron. Instead of the usual padding attenuator of 16–20 db, a $\pi/4$ rotator was inserted between oscillator and load. This element allows energy transport unilaterally and is capable of providing the necessary decoupling without introducing attenuation. The $\pi/4$ Faraday rotator is one of the interesting technical applications of the Faraday rotation of guided waves at microwave frequencies. Its action can be understood from fig. 2. A wave travelling from A to B is transmitted without attenuation when the analyzer is rotated $\pi/4$ radians and is thus adapted to the polarization of the wave emerging from the rotator. A wave travelling from B to A in the same system, however, arrives at the polarizer, which is now analyzer, with a direction of polarization which is $\pi/2$ out of the right direction for the wave to be transmitted. In fact it is completely absorbed by the absorbing vane. By means of a variable stub the $\pi/4$ rotator can be made a match for waves reflected at the

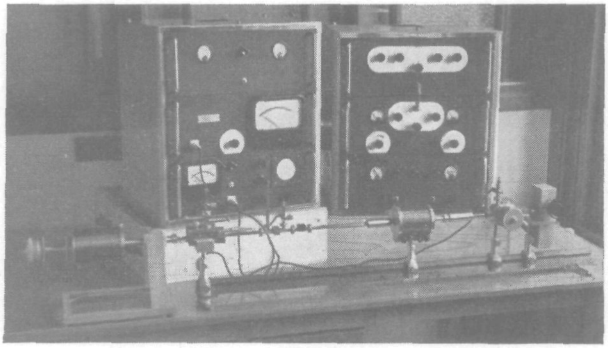

Fig. 14. Picture showing the wave guide system and the electronic equipment.

load. Thus we have in our measuring system an incident wave of constant amplitude carrying virtually all power produced by the klystron.

The actual measuring devices are a directional coupler, which is capable of measuring the amplitude of the reflected wave, and a standing wave detector which allows exploration of the standing wave pattern arising from the superposition of incident and reflected waves. A transmission type cavity wavemeter is connected to the line between oscillator and $\pi/4$ rotator. The output of the klystron is modulated by a 1000 Hz square wave modulation at the reflector. The detected signal then also is a square wave voltage, which either may be amplified by a 1000 Hz selective amplifier and read on a vacuum tube voltmeter or can be displayed at an oscilloscope. The electronic equipment contains a stabilized power supply for the klystron and a stabilized supply which serves the modulator, the selective amplifier and the oscilloscope. The time base sweep for the oscilloscope is taken from the modulator unit which can give both square wave and sawtooth modulation. The latter also permits an easy adjustment of the working potentials and the klystron tuning. Fig. 14 shows a picture of the apparatus.

Interpretation of experimental data. We shall now consider the question: how are the immediate experimental data, i.e. standing wave ratio, shift of standing wave pattern and amplitude of reflected wave, related to the physical quantities we want to measure. In particular one type of measurement will be

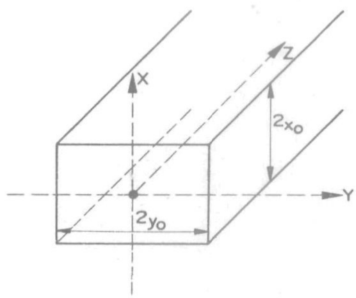

Fig. 15. Coordinate system in rectangular wave guide.

analyzed, viz. the study of the properties of cavity resonances. Before dealing with this application, however, let us first recall some properties of the fields in the measuring system. The wave guide permits none but the TE_{01}-mode. When the coordinates are chosen as in fig. 15, the total field will be a superposition of waves travelling in the directions $+z$ and $-z$. The transverse components of the first wave are in general

$$\left.\begin{aligned} E_x^i &= \hat{E}^i \exp(-j\beta z) \cos(\pi y/2y_0), \\ H_y^i &= (\hat{E}^i/Z_c) \exp(-j\beta z) \cos(\pi y/2y_0), \end{aligned}\right\} \quad (3.6)$$

and of the wave travelling in the direction $-z$

$$\left.\begin{aligned} E_x^r &= \hat{E}^r \exp(j\beta z) \cos(\pi y/2y_0), \\ H_y^r &= -(\hat{E}^r/Z_c) \exp(j\beta z) \cos(\pi y/2y_0), \end{aligned}\right\} \quad (3.7)$$

where the indices i and r mean incident, c.q. reflected; $\beta = \{\omega^2\varepsilon_0\mu_0 - (\pi/2y_0)^2\}^{\frac{1}{2}}$ is the propagation constant of the TE_{01}-mode, and $Z_c = \omega\mu/\beta$ is the characteristic impedance for this mode. It is easily verified that these expressions are special forms of (1.11). By superposition we obtain

$$\left.\begin{aligned} E_x &= \hat{E}^i \exp(-j\beta z)\,\{1 + r(z)\}\cos(\pi y/2y_0), \\ H_y &= (\hat{E}^i/Z_c)\exp(-j\beta z)\,\{1 - r(z)\}\cos(\pi y/2y_0), \end{aligned}\right\} \tag{3.8}$$

where

$$r(z) = (\hat{E}^r/\hat{E}^i)\exp(2j\beta z) = r(0)\exp(2j\beta z). \tag{3.9}$$

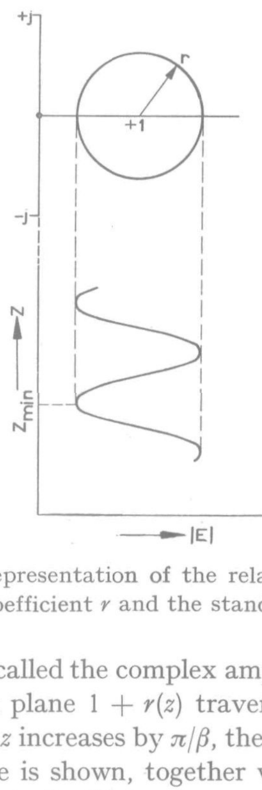

Fig. 16. Representation of the relation between the reflection coefficient r and the standing wave pattern.

The quantity $r(z)$ is called the complex amplitude reflection coefficient. In the complex plane $1 + r(z)$ traverses a circle around the centre $+1$. Each time z increases by π/β, the circle is traversed once. In fig. 16 such a circle is shown, together with the standing wave pattern corresponding to it: $|E|$ has been plotted against z. Clearly the standing wave ratio η is related to $|r|$ by

$$\eta = E_{max}/E_{min} = (1 + |r|)/(1 - |r|), \tag{3.10}$$

which is equivalent to

$$|r| = (\eta - 1)/(\eta + 1). \tag{3.11}$$

In a standing wave minimum r is negative real, $r(z_{min}) = -|r|$, and on account of (9) and (11) we find for the reflection coefficient in an arbitrary point z

$$r(z) = r(z_{min}) \exp\{2j\beta(z - z_{min})\} =$$
$$= \{(1-\eta)/(1+\eta)\} \exp\{2j\beta(z - z_{min})\}. \quad (3.12)$$

Thus we see that $r(z)$ is completely determined by η and z_{min}. The reflection coefficient is related to the impedance $Z(z) = E_x(z)/H_y(z)$ in a simple way. Dividing the equations (8) by each other we find immediately

$$Z(z)/Z_c = \{1 + r(z)\}/\{1 - r(z)\}. \quad (3.13)$$

Keeping in mind that $r(z_{min}) = -|r|$, and that in a standing wave maximum $r(z_{max}) = +|r|$, we find from (11) and (13)

$$Z(z_{max})/Z_c = \eta, \quad (3.14)$$

$$Z(z_{min})/Z_c = 1/\eta. \quad (3.15)$$

From this analysis we may conclude that we can determine both $r(z)$ and $Z(z)/Z_c$ at all points of the line by measuring the standing wave ratio η and the position of a standing wave minimum z_{min}. We shall now consider the application mentioned above which is related to our own measurements.

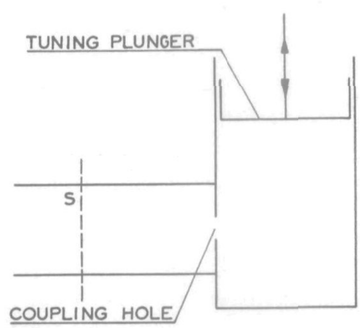

Fig. 17. Schematic drawing of cavity and reference plane S.

S t u d y o f c a v i t y r e s o n a n c e s. We wish to investigate the system consisting of a wave guide terminated by a tunable cavity (see fig. 17). The cavity may be coupled to the wave guide by means of one or more holes. It can be proved (cf. S l a t e r [26])) that in a plane S in the wave guide the impedance $Z(\omega)$ in the neighbourhood of a resonance frequency is given by the expression

$$\frac{Z(\omega)}{Z_c} = \frac{1/Q_{ext}}{j(\omega/\omega_0 - \omega_0/\omega) + 1/Q_0} + \frac{Z_s}{Z_c}, \tag{3.16}$$

where Q_0 is the so-called unloaded Q, being the Q of a completely enclosed cavity of the same size. Different choices of the position of S result in different values of Q_{ext} and Z_s. The impedance Z_s is virtually constant in a narrow frequency range around a resonance

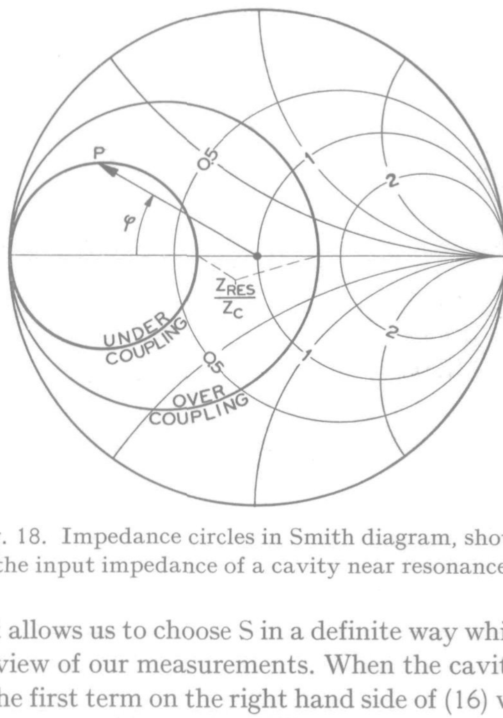

Fig. 18. Impedance circles in Smith diagram, showing the input impedance of a cavity near resonance.

and this fact allows us to choose S in a definite way which is especially useful in view of our measurements. When the cavity is tuned off resonance, the first term on the right hand side of (16) will disappear, and the impedance $Z(\omega) \simeq Z_s$. Off resonance only a very small amount of power will be absorbed by the cavity, and this will result in a very high standing wave ratio in the feeding wave guide. It is then clear from (15) that we can make Z_s very small by letting S coincide with a minimum in the standing wave pattern. In that case

$$Z_s/Z_c \simeq 1/\eta_1 \ll 1. \tag{3.17}$$

We shall neglect the second term in (16) from now on, where it is to be understood that we have chosen S in the proper way. Let us next investigate the representation of (16) in the Smith-chart; this, as is well-known, is a reflection coefficient plane on which lines of constant real and imaginary part of reduced impedance Z/Z_c have been drawn (see fig. 18). On account of (13), (16) and a property of bilinear transformations, the representation of $Z(\omega)$ in the Smith-chart is a circle which is symmetrical with respect to the real axis. Off resonance $Z = 0$; at resonance $Z_{res}/Z_c = Q_0/Q_{ext}$. Thus the two points where the circle intersects the real axis are fixed, and therefore the circle itself is completely determined. In fig. 18 two such circles have been drawn, one for $Q_0 < Q_{ext}$, the other for $Q_0 > Q_{ext}$. The first does not include the point $Z/Z_c = 1$, the second does.

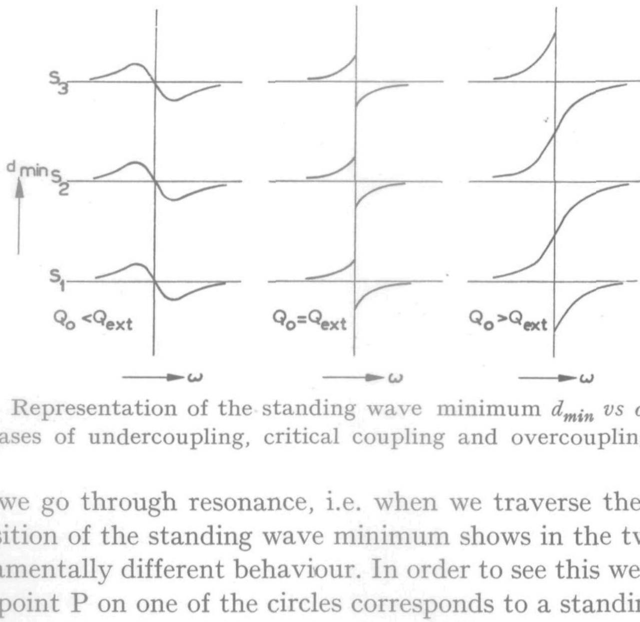

Fig. 19. Representation of the standing wave minimum d_{min} *vs* ω for the cases of undercoupling, critical coupling and overcoupling.

When we go through resonance, i.e. when we traverse the circles, the position of the standing wave minimum shows in the two cases a fundamentally different behaviour. In order to see this we remark that a point P on one of the circles corresponds to a standing wave pattern in which the minimum has been shifted with respect to S over a distance $d = \varphi/2\beta$ as is evident from what we have seen above concerning $r(z)$: we must move over the distance $d = \varphi/2\beta$ to arrive at a point of negative real r, which occurs at a standing wave minimum. Now it is clear that, if we traverse the circle for $Q_0 < Q_{ext}$, φ goes through a maximum and a minimum, finally returning to its original value $\varphi = 0$; for $Q_0 > Q_{ext}$, however, φ_0 increases by 2π, resulting in a shift $d = \lambda_g/2$. This behaviour is illustrated in fig. 19, where d has been plotted against ω.

We are thus led to distinguish three cases:

a) $Z_{res}/Z_c < 1$; $Q_0 < Q_{ext}$; undercoupling. At resonance S still coincides with a standing wave minimum, and in view of (15) we have

$$Q_0/Q_{ext} = Z_{res}/Z_c = 1/\eta_{res}. \tag{3.18}$$

b) $Z_{res}/Z_c = 1$; $Q_0 = Q_{ext}$; critical coupling. At resonance the cavity absorbs all incident power.

c) $Z_{res}/Z_c > 1$; $Q_0 > Q_{ext}$; overcoupling. Here the plane S no longer coincides with a minimum at resonance but with a maximum (see fig. 19). Therefore

$$Q_0/Q_{ext} = Z_{res}/Z_c = \eta_{res}. \tag{3.19}$$

Thus we see that we can find the ratio Q_0/Q_{ext} by measuring η_{res}; we must observe the shift of the minimum in the standing wave pattern to distinguish between the cases of overcoupling and undercoupling. We usually want to know Q_0 separately, and then evidently another relation is needed. We shall now show that such additional information can be obtained by means of the directional coupler.

The power flow in the incident wave is S_0; the ratio of reflected and incident power is

$$S_r/S_0 = R = rr^*. \tag{3.20}$$

From (13) it is easily derived that

$$r = (Z - Z_c)/(Z + Z_c) = (Y_c - Y)/(Y_c + Y). \tag{3.21}$$

Because of (16)

$$Y/Y_c = Q_{ext}/Q_0 + jv\, Q_{ext}, \tag{3.22}$$

where $v = \omega/\omega_0 - \omega_0/\omega$. Substituting (22) into (21), and (21) into (20) we find

$$\frac{S_r}{S_0} = 1 - \frac{4Q_{ext}/Q_0}{(1 + Q_{ext}/Q_0)^2 + v^2 Q_{ext}^2} = 1 - \frac{S_a}{S_0}, \tag{3.23}$$

where S_a/S_0 is the ratio of absorbed to incident power. The absorption is a maximum for $v = 0$; the half power points are given by

$$v = \pm\, (1/Q_{ext} + 1/Q_0) = \pm\, 1/Q_L. \tag{3.24}$$

The quantity Q_L is commonly called loaded Q and equals $Q_L = \omega_0/2\Delta\omega$, where $\Delta\omega$ is the frequency shift necessary to make the absorbed power 50% of the power absorbed at resonance. Eliminating Q_{ext} between (24), (18) and (19) we finally obtain the relations

$$\left.\begin{array}{ll} Q_0 = Q_L(1 + 1/\eta_{res}) & \text{undercoupling,} \\ Q_0 = 2Q_L & \text{critical coupling,} \\ Q_0 = Q_L(1 + \eta_{res}) & \text{overcoupling.} \end{array}\right\} \quad (3.25)$$

In other words: in order to find Q_0 it is sufficient to measure Q_L and η_{res}.

Table II shows some experimental results for a cylindrical K-band cavity, coupled to a rectangular wave guide by means of two circular holes (see fig. 12). The diameter of the cavity is 1 cm. For a series of hole diameters d we have listed η_{res}, Q_L, Q_0, Q_{ext} and the ratio of the power absorbed at resonance S_{max} and the incident power S_0. The series includes examples of both overcoupling and undercoupling.

TABLE II

d mm	Type of coupling	η_{res}	Q_L	Q_0	Q_{ext}	S_{max}/S_0
3.6	overcoupling	2.04	1128	3420	1690	0.90
3.4	,,	1.21	1535	3390	2800	0.99
3.2	undercoupling	1.49	1859	3100	4640	0.97
3.0	,,	2.36	2172	3090	7310	0.84
2.8	,,	4.15	2744	3420	13900	0.57
2.6	,,	6.04	3030	3530	21400	0.41
2.4	,,	9.41	2880	3190	29600	0.27

§ 10. *The materials investigated.* The materials investigated are the Ferroxcubes IVA, B, C, D, E. They are nickel zinc ferrites, containing nickel and zinc in different proportions, and they are usually furnished as ceramics. On account of the sintering process by which they are made, a certain porosity always remains, varying from a few percent for the very dense specimens up to about 30 percent for the very porous ones. Table III shows the values of some physical constants of the media used in our experiments.

The values of the specific gravity and of the coercive force have been taken from our own measurements. The other values have been derived from data by Gorter and Went [35]) and of Wijn [36]) on the assumption that the saturation magnetization is proportional to the density of the material. The values of μ_i are average production data.

TABLE III

Ferroxcube	Chemical composition in mol %		Specific gravity	Saturation magnetization 10^{-4} Wb/m^3	Porosity %	Initial perm. μ_i/μ_0	Coercive force 100 A/m
	NiO	ZnO					
IVA	17.5	33.2	4.45	3360	16.6	650	1
IVB	24.9	24.9	4.80	4400	11.0	230	0.5
IVC	31.7	16.5	4.52	4365	16.2	90	3.5
IVD	39.0	9.4	3.98	3470	26.2	45	8
IVE	48.2	0.7	3.80	2315	29.5	17	13

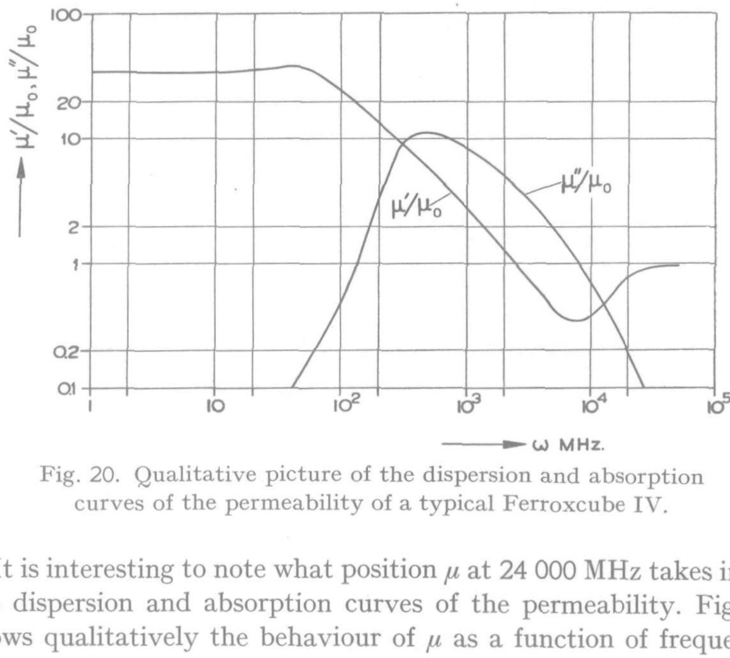

Fig. 20. Qualitative picture of the dispersion and absorption curves of the permeability of a typical Ferroxcube IV.

It is interesting to note what position μ at 24 000 MHz takes in on the dispersion and absorption curves of the permeability. Fig. 20 shows qualitatively the behaviour of μ as a function of frequency (cf. Polder [18]), Birks [5])). The dispersion and absorption can largely be interpreted as a ferromagnetic resonance in the anisotropy fields. Our working frequency is just above the dispersion region, and in the demagnetized state magnetic losses are negligible at 24 000 MHz. All measurements published hitherto have been performed at 10 000 MHz; at this frequency, however, considerable magnetic losses occur in the demagnetized state.

Preparation of the specimens. Our specimens were cylindrical rods, about 35 mm in length and with diameters ranging from 0.5 to 3 mm. The preparation of these rods is rather difficult on account of the hardness and the brittleness of the ferrites. They were ground on a special machine, designed and constructed by Mr P. Leemans of this laboratory. The essential element is drawn schematically in fig. 21.

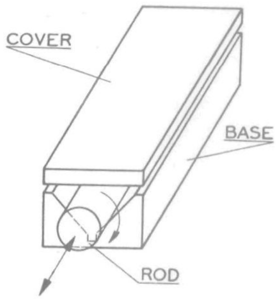

Fig. 21. Schematic drawing of grinder.

The rod is given both a rotational and an axial movement through a grinder which consists of a V-shaped base and a cover. The surface of the grinder consists of diamond powder in araldite. The cover can be pressed on to the specimen with variable force, depending on its hardness and diameter. The main difficulty arises in connecting the rod with the driving mechanism. Without precautions there will be bending moments on the ferrite rods, as its axis does not coincide continuously with the driving axis, and breakage will occur. The problem was solved by using a driving shaft connected to both sides by means of small universal joints.

CHAPTER IV. EXPERIMENTAL RESULTS

The last two chapters will be devoted to a survey of our experimental results and the interpretation thereof. Although some data have been taken at a frequency of 10 000 MHz, we shall discuss here only the experiments that have been performed at 24 000 MHz. From what we have seen above concerning the frequency spectrum of the permeability it will be clear that the theory developed in Chapter II (in which the media were supposed to be without dissipation) applies very well to K-band experiments, but not to X-band experiments. The following quantities have been determined for the Ferroxcube IV-series:

a) The propagation constants γ_+ and γ_- and the Faraday rotation Θ as a function of an applied constant magnetic field (when starting from the demagnetized state) and of the radius of the rods.

b) Q-values of resonances for both circularly polarized component waves.

c) Hysteresis of the Faraday rotation.

§ 11. *The measurements. a*) The Faraday rotation per unit length. This was obtained from measurements of the wavelengths $\lambda_{g\pm}$ for the circularly polarized waves. From (3.5) we have

$$\Theta = \tfrac{1}{2}(\beta_+ - \beta_-) = \pi(1/\lambda_{g+} - 1/\lambda_{g-}). \qquad (4.1)$$

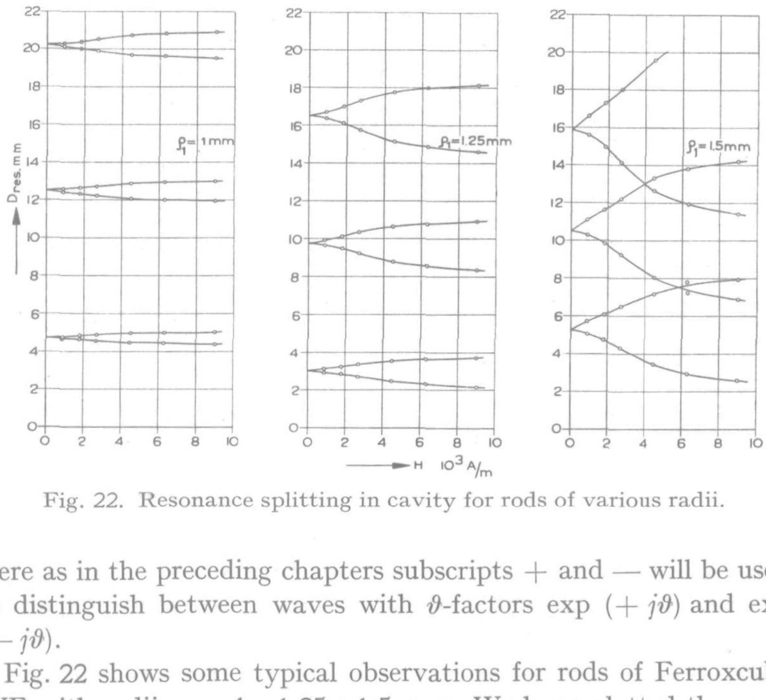

Fig. 22. Resonance splitting in cavity for rods of various radii.

Here as in the preceding chapters subscripts + and — will be used to distinguish between waves with ϑ-factors exp $(+ j\vartheta)$ and exp $(- j\vartheta)$.

Fig. 22 shows some typical observations for rods of Ferroxcube IVE with radii $\varrho_1 = 1$; 1.25 ; 1.5 mm. We have plotted the position for resonance D_{res} *vs.* the applied constant magnetic field. The resonance splitting rapidly increases with increasing radius, and for $\varrho_1 = 1.5$ mm the branches even overlap.

Fig. 23 contains sets of curves showing the magnetization M and the Faraday rotation Θ as functions of the applied magnetic field.

The upper diagrams refer to rods with $\varrho_1 = 0.5$ mm, the lower to rods with $\varrho_1 = 1$ mm. The indices A tot E indicate the different varieties of the Ferroxcube IV series. One notices immediately the striking

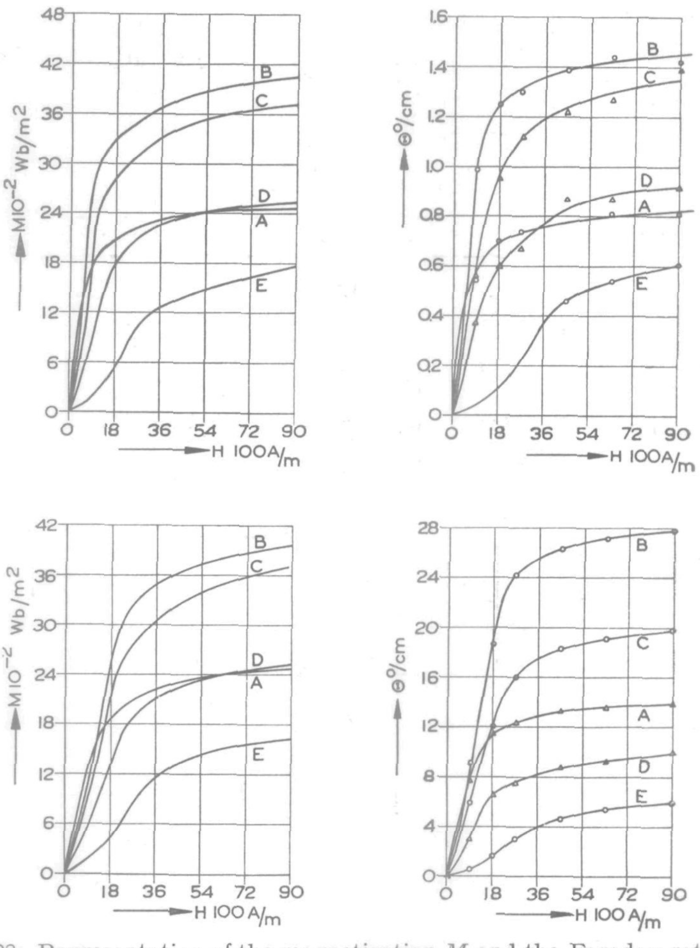

Fig. 23. Representation of the magnetization M and the Faraday rotation Θ *vs* the applied constant magnetic field. The upper diagrams refer to rods with $\varrho_1 = 0.5$ mm, the lower to rods with $\varrho_1 = 1.0$ mm.

resemblance between the two sets of curves in the upper diagrams, whereas the resemblance between the lower diagrams is considerably less. A remark must be added here about the magnetization curves. We have measured M by a ballistic method for rods with radii $\varrho_1 = 1.5$ mm, and the sets of curves in fig. 23 have been obtained from the measured data by correcting for the demagnetizing effect.

Fig. 24 shows the Faraday rotation as a function of ϱ_1. In these curves we have taken the rotations which are found for an applied constant field of 9000 A/m, i.e. near magnetic saturation (cf. fig. 23). Evidently within the range of radii considered here the curves may be represented empirically by expressions of the form

$$\log \Theta = C_1 + C_2\, \varrho_1. \tag{4.2}$$

Table IV lists the values of C_1 and C_2 obtained from fig. 24.

TABLE IV

Ferroxcube	C_1	C_2
IVA	—1.37	2.50
IVB	—1.14	2.56
IVC	—0.99	2.24
IVD	—1.10	2.10
IVE	—1.19	2.00

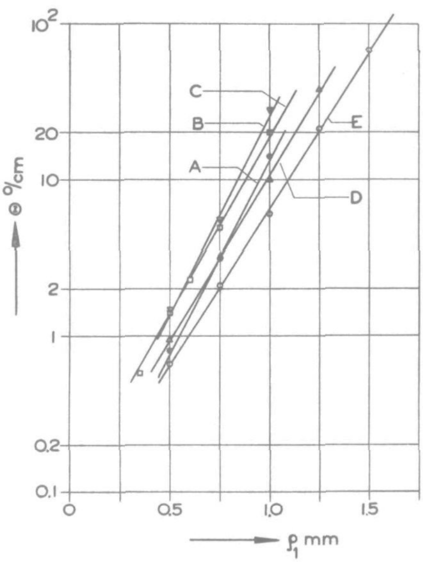

Fig. 24. Faraday rotation Θ *vs* rod diameter ϱ_1.

To facilitate comparison with the theory developed in chapter II and in particular with (2.118) we have plotted in fig. 25 the quantity

$10^{-6}\varrho_1^{-2}\,\Delta\beta$ against ϱ_1. This quantity, as we have seen, must approach a constant value when $\varrho_1 \to 0$. The radii used were $\varrho_1 = 0.5$; 0.75 ; 1 mm (for Ferroxcube IVC in addition rods with $\varrho_1 = 0.35$; 0.6 mm were employed). The middle curves refer to the ferrites in the demagnetized state and give $10^{-6}\,\varrho_1^{-2}\,\Delta\beta_0$; the upper and lower curves, representing $10^{-6}\varrho_1^{-2}\,\Delta\beta_\pm$, refer to the circularly polarized component waves when the materials are magnetized by a field of 9000 A/m. From fig. 25 it may be concluded that for $\varrho_1 > 0.5$ mm the approximation (2.118) is bad, whereas for $\varrho_1 < 0.5$ mm it is rather good. Unfortunately we could not use rods with radii smaller

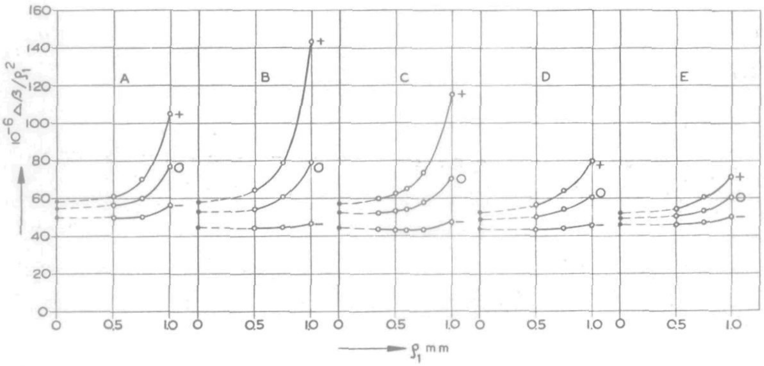

Fig. 25. Representation of $\Delta\gamma/\varrho_1^2$ against ϱ_1, cf. (2.118).

than $\varrho_1 = 0.35$—0.50 mm as the resonances of the right and left circularly polarized waves were no longer resolved. As pointed out earlier, however, this restriction is not a fundamental one since it is possible to excite the circularly polarized waves separately.

We now use the results collected in fig. 25 to find experimental values of μ_1 and μ_2. Evaluating the constants in (2.118) for our K-band cavity (inner diameter 1 cm) we obtain

$$10^{-6}\,\varrho_1^{-2}\,\Delta\beta_\pm = 28.5\,\frac{\mu_1 \pm \mu_2 - \mu_0}{\mu_1 \pm \mu_2 + \mu_0} + 60.2\,\frac{\varepsilon - \varepsilon_0}{\varepsilon + \varepsilon_0}. \qquad (4.3)$$

In the demagnetized state $\mu_1/\mu_0 \simeq 1$ (cf. fig. 20) and $\mu_2 = 0$, and instead of (3) we find

$$10^{-6}\,\varrho_1^{-2}\,\Delta\beta_0 = 60.2\,\frac{\varepsilon - \varepsilon_0}{\varepsilon + \varepsilon_0}. \qquad (4.4)$$

TABLE V

Ferroxcube	$\varepsilon/\varepsilon_0$	$\dfrac{\Delta\beta_+ - \Delta\beta_0}{10^6\varrho_1{}^2}$	$\dfrac{\Delta\beta_0 - \Delta\beta_-}{10^6\varrho_1{}^2}$	μ_1/μ_0	μ_2/μ_0
IVA	22	4 ± 0.4	5 ± 0.5	1.01 ± 0.03	0.31 ± 0.03
IVB	16	7 ± 0.7	8 ± 0.8	1.10 ± 0.06	0.54 ± 0.05
IVC	15	6 ± 0.6	8 ± 0.8	1.05 ± 0.05	0.49 ± 0.05
IVD	10	4 ± 0.4	5 ± 0.5	1.01 ± 0.03	0.31 ± 0.03
IVE	10	2.5 ± 0.25	3.5 ± 0.35	0.98 ± 0.02	0.20 ± 0.01

Extrapolating the middle curves in fig. 25 towards $\varrho_1 = 0$ we can use (4) to determine the values of ε listed in table V. This table also contains experimental values of the quantities

$$\frac{\Delta\beta_+ - \Delta\beta_0}{10^6\,\varrho_1^2} = 28.5\,\frac{\mu_1+\mu_2-\mu_0}{\mu_1+\mu_2+\mu_0} \text{ and } \frac{\Delta\beta_0 - \Delta\beta_-}{10^6\,\varrho_1^2} = -28.5\,\frac{\mu_1-\mu_2-\mu_0}{\mu_1-\mu_2+\mu_0} \quad (4.5)$$

obtained by extrapolating the upper and lower curves in fig. 25. With the help of (5) one easily derives the values of μ_1 and μ_2 shown in the last two columns of table V. The maximum possible error in the value of (5) due to the extrapolations is $\pm$ 10%. Table V also shows these errors and the resulting uncertainties in μ_1 and μ_2.

b) A t t e n u a t i o n. In order to find the attenuation to be expected in a Faraday rotator we performed some Q-measurements as described in the preceding chapter. Until now we had supposed the propagation constants γ to be imaginary. In fact they have a small real part: $\gamma = \alpha + j\beta$, where $\alpha/\beta \ll 1$. The attenuation constant α can be shown to be related to Q_0 according to the expression (cf. S l a t e r [26]), Chapter III)

$$\alpha = \frac{\omega}{2Q_0 v_g} = \frac{\omega}{2Q_0\,\mathrm{d}\omega/\mathrm{d}\beta}. \quad (4.6)$$

As $\mathrm{d}\omega/\mathrm{d}\beta$ cannot be obtained theoretically in a simple way, we determined its value experimentally by measuring β at two slightly different frequencies. Table VI lists the results of the Q- and α-measurements as functions of H_c for a rod of Ferroxcube IVB with $\varrho_1 = 1$ mm. Moreover it contains values of attenuations in db/cm, which are numerically equal to $0.2\,\alpha$, as is easily verified.

The α's listed here will be somewhat too large. This is due to the fact that (6) only applies when the losses in the end plates of the cavity may be neglected in comparison with the losses in the cylinder wall and the ferrite rod. The losses in the ferrite are so small, however,

TABLE VI

H_c A/m	Q_{0+}	Q_{0-}	α_+	α_-	db$^+$/cm	db$^-$/cm
0	1380		0.35		0.07	
765	1360	1375	0.37	0.33	0.07	0.07
1125	1365	1490	0.41	0.29	0.08	0.06
1350	1345	1570	0.42	0.28	0.08	0.06
1575	1470	1485	0.41	0.29	0.08	0.06
1800	1415	1515	0.44	0.28	0.09	0.06
2250	1390	1610	0.46	0.27	0.09	0.05
2700	1500	1640	0.44	0.27	0.09	0.05
3600	1430	1660	0.51	0.26	0.10	0.05
5400	1380	1620	0.53	0.26	0.11	0.05
9000	1440	1530	0.53	0.26	0.11	0.05

that this condition is not fulfilled. The error in α is probably of the order of 10—20%.

c) Hysteresis. There are two reasons for measuring the hysteresis of the Faraday rotation. First there is the technical reason that it might be possible to use the remanent magnetization in the

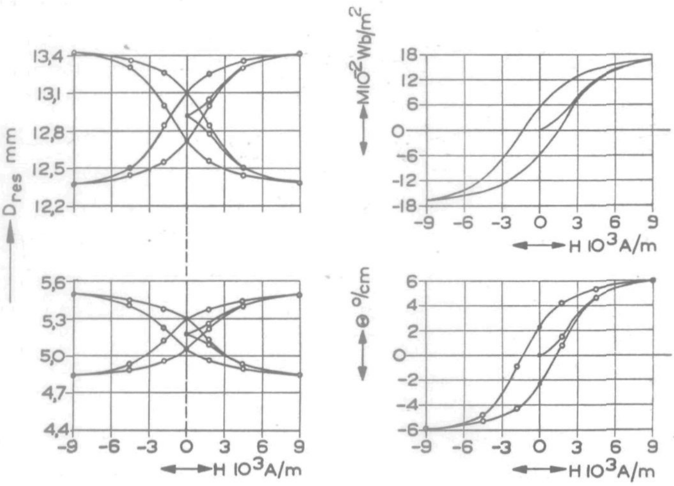

Fig. 26. Hysteresis of magnetization and Faraday rotation.

realisation of microwave circuit elements that violate the reciprocity theorem (cf. § 3). Secondly there is the physical reason that it is interesting to verify Rado's theory of the permeability tensor in non-saturated ferrites (cf. chapter V).

Fig. 26 shows some observations on a rod of Ferroxcube IVE with

$\varrho_1 = 1$ mm and the Faraday rotations derived from these measurements. It also shows the magnetic hysteresis curve measured for the same material. Evidently there is much resemblance between the two hysteresis curves. In table VII we have listed experimental values of M_{rem}/M_{max} and $\Theta_{rem}/\Theta_{max}$, representing the ratio of the remanent magnetization (c.q. Faraday rotation) and the saturation value. Table VII also contains H_{cm} and H_{cf}, the coercive forces for magnetization, c.q. Faraday rotation. The values for the Ferroxcubes IVA and B just indicate the order of magnitude.

TABLE VII

Ferroxcube	M_{rem}/M_{max}	$\Theta_{rem}/\Theta_{max}$	H_{cm} A/m	H_{cf} A/m
IVA	0.03	0.04	100	100
IVB	0.03	0.02	50	150
IVC	0.06	0.09	350	300
IVD	0.17	0.27	800	900
IVE	0.34	0.37	1300	1300

It may be concluded, however, that there is rather good agreement between the behaviour of magnetization and Faraday rotation. From the column giving $\Theta_{rem}/\Theta_{max}$ it is seen that the remanent rotation of IVD and E may be technically useful.

§ 12. *Some remarks on the accuracy of the measurements.* Let us first investigate the possible experimental error when we measure Faraday rotations. We determine Θ from the relation $\Theta = \frac{1}{2}(\beta_+ - \beta_-) = 180\,(1/\lambda_{g+} - 1/\lambda_{g-})$. In practice we measure $\frac{1}{2}\lambda_{g\pm}$ by observing the positions of two subsequent resonances. The possible error in D_{res} is $\delta D_{res} = 10^{-4}$ cm. Then $\delta\lambda_g = 4 \times 10^{-4}$ cm. For $\lambda_g \simeq 1.5$ cm we then find from the expression for Θ given above

$$\delta\Theta \simeq 0.07\ ^0/\text{cm}.$$

This error is only important when we want to measure very small Faraday rotations, as shown in the upper graph of fig. 23. Next to this experimental error there are some other sources of inaccuracies which arise from the fact that the specimens always show certain imperfections. The material can be slightly inhomogeneous on account of the sintering, and the specimens may be slightly conical instead of cylindrical. The influence of the last effect can be estimated from fig. 24. Another source of errors is the variation of the magnetic field along the axis of the coil in which the ferrite rod is placed. Measurements with a flip coil have shown that over the length of the rods the field is constant to within $\pm$ 1%.

CHAPTER V. PHYSICAL INTERPRETATION OF EXPERIMENTAL DATA

In order to arrive at a physical interpretation of our experimental results we shall first discuss Polder's and Rado's theories of the permeability tensor of magnetized substances. Polder dealt with the case of saturated ferromagnetics and covered the field of ferromagnetic resonance phenomena. Rado recently extended this theory to include non-saturated media as well. The latter considerations are of special interest in connection with the Faraday rotation of guided waves. In the following pages we shall derive expressions for the elements of the permeability tensor and compare these results with our experimental data.

§ 13. *Theory of the permeability tensor.* We describe a ferromagnetic substance as being composed of small domains in which electron spins are directed parallelly. Electron spins have both a magnetic dipole moment **m** and an angular momentum **L**. These quantities are proportional to each other:

$$\mathbf{m}/\mathbf{L} = \Gamma, \tag{5.1}$$

where Γ is the so-called gyromagnetic ratio. The parallel spins inside a domain give rise to a magnetization per unit volume which equals the saturation magnetization M_0. In demagnetized ferromagnetics the magnetizations of the different domains are oriented at random and no net magnetization results; if we apply a constant magnetic field to the material, however, a net magnetization arises in the direction of the applied field. In the boundary between two domains, a so-called Bloch wall, the orientation of the spins may be thought to change gradually from the spin direction on one side to the spin direction at the other side of the wall. We now wish to study the behaviour of the magnetization in these domains as well as of the bulk magnetization when in addition to the constant magnetic field H_c a h.f. electromagnetic field acts on the medium. We make the following assumptions and restrictions:

a) The volume of the Bloch walls can be neglected compared with the total volume;

b) The Bloch walls do not move under influence of the h.f. field. This condition is satisfied for all ferrites in the microwave region.

c) Three types of fields contribute to the static field distribution: the applied constant field $\mathbf{H}_c$, the demagnetizing fields $\mathbf{H}_d$, arising from the poles at the Bloch walls, and the anisotropy fields $\mathbf{H}_a$. Thus we can write for the static field

$$\mathbf{H}_0 = H_0\,\mathbf{k}' = \mathbf{H}_c + \mathbf{H}_d + \mathbf{H}_a, \tag{5.2}$$

where $\mathbf{k}'$ is a unit vector; clearly H_0 and $\mathbf{k}'$ are functions of position. The magnetization is also directed along $\mathbf{k}'$: $\mathbf{M} = M_0\,\mathbf{k}'$.

d) The z-axis is taken in the direction of $\mathbf{H}_c$.

In order to find the elements of the permeability tensor we first derive the equation of motion for an electron spin in an arbitrary domain. When a magnetic field H is applied to a magnetic dipole $\mathbf{m}$, the dipole experiences a torque $\mathbf{m} \times \mathbf{H}$. On the other hand this torque equal $\mathrm{d}\mathbf{L}/\mathrm{d}t = \Gamma^{-1}\,\mathrm{d}\mathbf{m}/\mathrm{d}t$, where we have used (1). The equation of motion then clearly is

$$\mathrm{d}\mathbf{m}/\mathrm{d}t = \Gamma\,\mathbf{m} \times \mathbf{H}. \tag{5.3}$$

Multiplying by the number of spins per unit volume N, we obtain the equation of motion for the magnetization

$$\mathrm{d}\mathbf{M}/\mathrm{d}t = \Gamma\,\mathbf{M} \times \mathbf{H}. \tag{5.4}$$

Let us now consider a magnetic field consisting of the static field (2) and a h.f.field $\mathbf{H}_1 \exp j\omega t$, where $|\mathbf{H}_1| \ll H_0$:

$$\mathbf{H} = H_0\mathbf{k}' + \mathbf{H}_1 \exp j\omega t. \tag{5.5}$$

The magnetization then will have the form

$$\mathbf{M} = M_0\mathbf{k}' + \mathbf{M}_1 \exp j\omega t. \tag{5.6}$$

On substituting (5) and (6) into (4) we obtain

$$j\omega\mathbf{M}_1 = \Gamma\,(H_0\mathbf{M}_1 - M_0\mathbf{H}_1) \times \mathbf{k}'. \tag{5.7}$$

Here we have neglected $\mathbf{M}_1 \times \mathbf{H}_1$ as it is small of second order.

We introduce an auxiliary system of Cartesian coordinates determined by the unit vectors $\mathbf{i}'$, $\mathbf{j}'$, $\mathbf{k}'$ as illustrated in fig. 27. $\mathbf{i}'$ lies in the $\mathbf{i}$, $\mathbf{j}$ plane. Writing

$$\mathbf{M}_1 = M_{1x'}\,\mathbf{i}' + M_{1y'}\,\mathbf{j}' + M_{1z'}\,\mathbf{k}' \text{ and } \mathbf{H}_1 = H_{1x'}\,\mathbf{i}' + H_{1y'}\,\mathbf{j}' + H_{1z'}\,\mathbf{k}'$$

we find from (7)

$$M_{1x'} = \mu_0(\chi_1' H_{1x'} - j\chi_2' H_{1y'}),\ M_{1y'} = \mu_0(j\chi_2' H_{1x'} + \chi_1' H_{1y'}),\ M_{1z'} = 0, \tag{5.8}$$

where

$$\mu_0 \chi_1' = \frac{\Gamma^2 M_0 H_0}{\Gamma^2 H_0^2 - \omega^2}, \quad \mu_0 \chi_2' = \frac{\omega \Gamma M_0}{\Gamma^2 H_0^2 - \omega^2}. \tag{5.9}$$

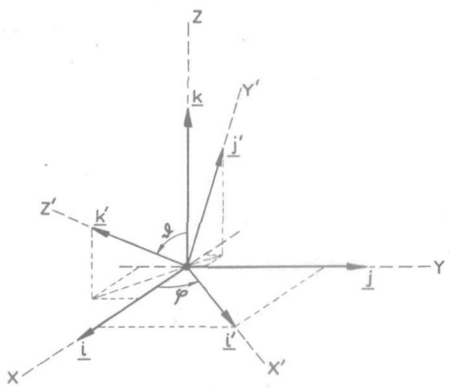

Fig. 27. Fixed and variable coordinate systems. The variable system is chosen in such a way that the z'-axis is directed along the magnetization, whereas the x'-axis lies in the xy-plane.

The x-, y-, and z-components of $\mathbf{M}_1$ can be found from the identity

$$\mathbf{M}_1 = M_{1x'}\,\mathbf{i}' + M_{1y'}\,\mathbf{j}' = M_{1x}\,\mathbf{i} + M_{1y}\,\mathbf{j} + M_{1z}\,\mathbf{k}.$$

In a straightforward manner we can derive

$$\left.\begin{aligned}
M_{1x} = {} & \mu_0 \chi_1' (\cos^2 \varphi + \cos^2 \vartheta \sin^2 \varphi) H_{1x} + \\
& + \mu_0 (\chi_1' \sin^2 \vartheta \sin \varphi \cos \varphi - j\chi_2' \cos \vartheta) H_{1y} + \\
& + \mu_0 (- \chi_1' \sin \vartheta \cos \vartheta \sin \varphi - j\chi_2' \sin \vartheta \cos \varphi) H_{1z}, \\
M_{1y} = {} & \mu_0 (\chi_1' \sin^2 \vartheta \sin \varphi \cos \varphi + j\chi_2' \cos \vartheta) H_{1x} + \\
& + \mu_0 \chi_1' (\sin^2 \varphi + \cos^2 \vartheta \cos^2 \varphi) H_{1y} + \\
& + \mu_0 (\chi_1' \sin \vartheta \cos \vartheta \cos \varphi - j\chi_2' \sin \vartheta \sin \varphi) H_{1z}, \\
M_{1z} = {} & \mu_0 (- \chi_1' \sin \vartheta \cos \vartheta \sin \varphi + j\chi_2' \sin \vartheta \cos \varphi) H_{1x} + \\
& + \mu_0 (\chi_1' \sin \vartheta \cos \vartheta \cos \varphi + j\chi_2' \sin \vartheta \sin \varphi) H_{1y} \\
& + \mu_0 \chi_1' \sin^2 \vartheta\, H_{1z}.
\end{aligned}\right\} \tag{5.10}$$

These equations describe the x-, y-, and z-components of the h.f. magnetization in a very small volume, where the direction of the static field is given by the unit vector $\mathbf{k}'$. The macroscopic h.f. magnetization can be obtained in principle by averaging (10) over all directions $\mathbf{k}'$. Unfortunately we do not know in general the relative probability with which a certain direction $\mathbf{k}'$ occurs. We can reach some valuable conclusions, however. For a specimen with rotational symmetry around the z-axis (which is also the direction of the applied constant magnetic field) it follows from symmetry considerations that all values of φ between 0 and 2π have equal probabilities. Denoting the average of $\sin\varphi$ by $<\sin\varphi>$ we can then say that $<\sin\varphi> = <\cos\varphi> = <\sin\varphi\cos\varphi> = 0$; $<\sin^2\varphi> = <\cos^2\varphi> = \frac{1}{2}$. Thus we retain for the components of the macroscopic magnetization

$$\begin{aligned} <M_{1x}> &= \mu_0 <\chi_1'(\tfrac{1}{2} + \tfrac{1}{2}\cos^2\vartheta)> H_{1x} - j\mu_0 <\chi_2'\cos\vartheta> H_{1y}, \\ <M_{1y}> &= j\mu_0 <\chi_2'\cos\vartheta> H_{1x} + \mu_0 <\chi_1'(\tfrac{1}{2} + \tfrac{1}{2}\cos^2\vartheta> H_{1y}, \\ <M_{1z}> &= \mu_0 <\chi_1'\sin^2\vartheta> H_{1z}. \end{aligned} \tag{5.11}$$

These relations define a susceptibility tensor

$$\|\chi\| = \begin{Vmatrix} \chi_1 & -j\chi_2 & 0 \\ j\chi_2 & \chi_1 & 0 \\ 0 & 0 & \chi_3 \end{Vmatrix}, \tag{5.12}$$

where

$$\left.\begin{aligned} \chi_1 &= \frac{\Gamma^2 M_0}{\mu_0} < \frac{H_0}{\Gamma^2 H_0^2 - \omega^2}(\tfrac{1}{2} + \tfrac{1}{2}\cos^2\vartheta) >, \\ \chi_2 &= \frac{\omega\Gamma M_0}{\mu_0} < \frac{\cos\vartheta}{\Gamma^2 H_0^2 - \omega^2} >, \\ \chi_3 &= \frac{\Gamma^2 M_0}{\mu_0} < \frac{H_0}{\Gamma^2 H_0^2 - \omega^2}\sin^2\vartheta >. \end{aligned}\right\} \tag{5.13}$$

From (11) and (12), and the relation $\mathbf{B} = \mu_0\mathbf{H} + \mathbf{M}$ we obtain the permeability tensor

$$\|\mu\| = \begin{Vmatrix} \mu_1 & -j\mu_2 & 0 \\ j\mu_2 & \mu_1 & 0 \\ 0 & 0 & \mu_3 \end{Vmatrix}, \tag{5.14}$$

where $\mu_1 = \mu_0(1 + \chi_1)$; $\mu_2 = \mu_0\chi_2$; $\mu_3 = \mu_0(1 + \chi_3)$.

Let us now consider three special cases:

a) Demagnetized state. In this case all directions $\mathbf{k}'$ have equal probabilities so that $<\sin^2\vartheta> = 2/3$; $<\cos^2\vartheta> = 1/3$; $<\cos\vartheta> = 0$. Substituting these results in (13) we find

$$\chi_1 = \chi_3 = \chi = \frac{2}{3}\frac{\Gamma^2 M_0}{\mu_0} < \frac{H_0}{\Gamma^2 H_0^2 - \omega^2} >, \quad \chi = 0. \quad (5.15)$$

Thus, as we could expect, the medium is isotropic.

b) $-\Gamma H_0 \ll \omega$. In the numerators in (13) we neglect $\Gamma^2 H_0^2$ with respect to ω^2. We cannot say anything about χ_1 without making specific assumptions concerning the H_0- and ϑ-distributions. We can only state that at 24 000 MHz and for practical values of M_0 the susceptibilities $\chi_1 \ll 1$ and $\chi_3 \ll 1$, and therefore $\mu_1 \simeq \mu_3 \simeq \mu_0$. The result for χ_2, however, is interesting:

$$\chi_2 = -\frac{\Gamma}{\omega\mu_0} < M_0 \cos\vartheta > = -\frac{\Gamma M_z}{\omega\mu_0}, \quad (5.16)$$

i.e. the tensor element $\chi_2 = \mu_2/\mu_0$ is proportional to M_z, and in non-saturated ferromagnetics, in which the condition $-\Gamma H_0 \ll \omega$ is satisfied, μ_2 as a function of H_c is given by curves of the same shape as the magnetization and hysteresis curves. This is the result obtained bij Rado[19]).

c) The substance is magnetically saturated. Now $\cos\vartheta = 1$; $\sin\vartheta = 0$. This case was studied by Polder. If H_0 is the same at all points in the medium, we obtain from (13)

$$\chi_1 = \frac{\Gamma^2 M_0 H_0}{\mu_0(\Gamma^2 H_0^2 - \omega^2)}, \quad \chi_2 = \frac{\omega\Gamma M_0}{\mu_0(\Gamma^2 H_0^2 - \omega^2)}, \quad (5.17)$$

and the resonant denominator of these expressions forms the basis for an understanding of ferromagnetic resonance phenomena. It is immediately clear that there will be no sharply defined resonances in ferromagnetic specimens of arbitrary shape as H_0 is not the same at all points. In order to avoid this situation ferromagnetic resonance experiments should be performed on small single crystals of ellipsoidal or spherical form, in which the anisotropy and demagnetizing fields are the same all over the specimen.

In § 2 we considered the propagation of plane waves through media which are both gyromagnetic and gyroelectric. From the results obtained there we can derive the propagation constants for media which are gyromagnetic only. For the case of the magnetic Faraday effect we find effective permeabilities of the form $\mu_1 \pm \mu_2$. With the aid of (17) we obtain

$$\mu_1+\mu_2=\mu_0+\Gamma M_0/(\Gamma H_0-\omega),\ \mu_1-\mu_2=\mu_0+\Gamma M_0/(\Gamma H_0+\omega). \quad (5.18)$$

It is clear that as Γ is negative, $\mu_1 + \mu_2$ does not show resonance, whereas $\mu_1 - \mu_2$ becomes infinite for $\omega_r = -\Gamma H_0$. For the case of the magnetic Cotton-Mouton effect we have an effective permeability of the form $(\mu_1^2 - \mu_2^2)/\mu_1$. Here we find

$$\frac{\mu_1^2-\mu_2^2}{\mu_1} = \mu_0 \frac{\Gamma^2 (B_0/\mu_0)^2 - \omega^2}{\Gamma^2 H_0 B_0/\mu_0 - \omega^2} \quad (5.19)$$

with $B_0 = \mu_0 H_0 + M_0$. Now the resonance condition is $\omega_r = -\Gamma\sqrt{H_0 B_0/\mu_0}$; this is Kittel's result for flat discs [15]).

§ 14. *Experimental verification of Rado's theory*. We have seen above that according to Rado's theory in our case $\mu_1/\mu_0 \simeq 1$; $\mu_2/\mu_0 = -\Gamma M_z/\omega\mu_0$, where M is given in Wb/m^2, $\omega = 2\pi\times 24\times 10^9$ and $\Gamma = -0.220 \times 10^6$ m/As. Table VIII contains the theoretical values obtained from Rado's theory together with the experimental figures from Table V in Chapter IV. The agreement is seen to be good, taking into account the uncertainties of the experimental values.

TABLE VIII

Ferroxcube	Theory		Experiment	
	μ_1/μ_0	μ_2/μ_0	μ_1/μ_0	μ_2/μ_0
IVA	1	0.285	1.01 ± 0.03	0.31 ± 0.03
IVB	1	0.47	1.10 ± 0.06	0.54 ± 0.05
IVC	1	0.43	1.05 ± 0.05	0.49 ± 0.05
IVD	1	0.30	1.01 ± 0.03	0.31 ± 0.03
IVE	1	0.20	0.98 ± 0.02	0.20 ± 0.01

From (4.3) we find for the Faraday rotation introduced by thin rods

$$\Theta = \tfrac{1}{2}(\Delta\beta_+ - \Delta\beta_-) \simeq 14.2 \times 10^6 \varrho_1^2 \frac{\mu_2/\mu_0}{1-(\mu_2/2\mu_0)^2} \text{ rad/m}, \quad (5.20)$$

where ϱ_1 is expressed in meters. Therefore to a first approximation the Faraday rotation is proportional to μ_2, c.q. to M_z. The upper half of fig. 23 seems to be strong experimental evidence in support of this theoretical result: there is a close resemblance, indeed, between the two sets of curves referring to rods with $\varrho_1 = 0.5$ mm. The discrepancies between the sets of curves referring to rods with $\varrho_1 = 1$ mm must be due to the fact that (4.3) is then no longer a good approximation.

REFERENCES

1) Allen, P. J., Proc. Inst. Radio Engrs **41** (1953) 100.
2) Beljers, H. G., Physica **14** (1949) 629.
3) Berk, A. D. and B. Lax, Quarterly Progress Report M.I.T. July 15, 1952.
4) Berk, A. D. and B. Lax, Quarterly Progress Report M.I.T. Oct. 15, 1952.
5) Birks, J. B., Proc. Phys. Soc. London B **63** (1950) 65.
6) Born, M., Optik, Berlin 1933.
7) Gamo, H., J. Phys. Soc. Japan **8** (1953) 176.
8) Goldstein, L., M. A. Lampert and J. F. Heney, Elect. Commun. **28** (1951) 322.
9) Goldstein, L. and M. A. Lampert, Elect. Commun. **30** (1953) 164.
10) Hafner, E., Arch. elektr. Übertragung **7** (1953) 47.
11) Hogan, C. L., Bell Syst. Tech. J. **31** (1952) 1.
12) Jahnke, E. and F. Emde, Tables of functions, Leipzig 1933.
13) Kales, M. L., N.R.L. Report 4027, Aug. 8, 1952.
14) Kennelly, A. E., Chart Atlas of Complex Hyperbolic and Circular Functions, 1914.
15) Kittel, C., Phys. Rev. **73** (1948) 155.
16) Olin, I. D., Proc. Inst. Radio Engrs **41** (1953) 10.
17) Polder, D., Phil. Mag. **40** (1949) 100.
18) Polder, D., Proc. Instn. Elect. Engrs (London) II **97** (1950) 246.
19) Rado, G. I., Phys. Rev. **89** (1953) 529.
20) Reggia, F. and R. W. Beatty, Proc. Inst. Radio Engrs **41** (1953) 93.
21) Roberts, F. F., J. Phys. Radium **12** (1952) 305.
22) Rybner, J., Nomograms of Complex Hyperbolic Functions, Copenhagen 1947.
23) Sakiotis, N. G. and H. N. Chait, Proc. Inst. Radio Engrs **41** (1953) 87.
24) Schelkunoff, S. A., Proc. Inst. Radio Engrs **25** (1937) 1457.
25) Schelkunoff, S. A., Bell Syst. Tech.J. **31** (1952) 784.
26) Slater, J. C., Microwave Electronics, New York 1950.
27) Slater, J. C., Microwave Transmission, New York 1942.
28) Smullin, L. D., Quarterly Progress Report M.I.T. July 15, 1952.
29) Suhl, H. and L. R. Walker, Phys. Rev. **86** (1952) 122.
30) Tellegen, B. D. H., Philips Res. Rep. **3** (1948) 81.
31) Trier, A. A. Th. M. van, Phys. Rev. **87** (1952) 227.
32) Trier, A. A. Th. M. van, Appl. sci. Res. B **3** (1953) 142.
33) Trier, A. A. Th. M. van, Tijdschr. Ned. Radiogen. **18** (1953) 211.
34) Voigt, W., Magneto- und Elektrooptik, Leipzig 1908.
35) Went, J. J. and E. W. Gorter, Philips Techn. Tijdschr. **13** (1951) 213.
36) Wijn, H. P. J., thesis Leiden 1953.

Smidde '58

STELLINGEN

I

De dimensie-resonantie, die door Sakiotis en Chait beschouwd wordt als mogelijke oorzaak van het maximum in de tussenschakeldemping van een Faraday-rotator bij kleine magneetvelden, kan als zodanig worden uitgesloten.

Sakiotis, N. G. en H. N. Chait, Proc. I. R. E. **41** (1953) 93.

II

Om de vierpoolconstanten van niet-reciproke vierpolen te bepalen moet men behalve de kortsluit- en nullastimpedanties ook de verhouding van de tussenschakeldempingen in beide richtingen meten.

v. Trier, A. A. T. M., T. Ned. Radiogen. **18** (1953) 211.

III

De opmerking van Young en Uehling, dat in een trilholte, die een gyromagnetische wand bevat, twee afzonderlijke bijdragen tot Q^{-1} geleverd worden door de circulair gepolariseerde golven, waarin de golf in de trilholte kan worden ontbonden, is onjuist.

Young, J. A. en E. A. Uehling, Phys. Rev. **90** (1953) 990.

IV

In het gebied van de microgolven kan de diëlectrische constante van vaste stoffen, die een ε hebben van de orde van grootte 10, met voordeel gemeten worden aan dunne ronde staafjes, die coaxiaal worden aangebracht in een trilholte van ronde doorsnede.

V

In de discussie van ferromagnetische resonantie-experimenten door Yager e. a. wordt gebruik gemaakt van een door Kittel ingevoerde susceptibiliteit. Het verband tussen het imaginaire deel van deze susceptibiliteit en de resonantie-absorptie, dat door Yager wordt aangenomen, dient nader te worden toegelicht.

Yager, W. A. et al., Phys. Rev. **80** (1950) 744.
Kittel, Ch., Phys. Rev. *73*, (1948) 155.

VI

Het wetenschappelijke karakter van de informatietheorie wordt al te vaak geweld aangedaan door gekunstelde analogiebeschouwingen over processen, die in de levende natuur optreden, enerzijds en physische verschijnselen anderzijds.

VII

In verband met de toenemende industrialisatie in ons land behoeft de opleiding van instrumentmakers dringend een reorganisatie. Het is wenselijk deze opleiding wettelijk te regelen en een aantal erkende diploma's, corresponderend met verschillende graden van practische en theoretische bekwaamheid, in te voeren. Het laatste zou tevens kunnen leiden tot een juister onderscheid in maatschappelijke positie van geschoolden en ongeschoolden.

VIII

Het belang van militaire research op technisch en physisch gebied, als onderdeel van een defensieprogramma, wordt in Nederland zowel van militaire als van civiele zijde nog steeds onderschat.

IX

Het verdient aanbeveling een zekere mate van reclame in de televisie-programma's toe te staan.

X

Emigratie van Nederlandse boeren naar Ierland zou in het belang zijn van beide landen.